OPTICALLY STIMULATED LUMINESCENCE STUDIES ON NATURAL FLUORITES

A THESIS SUBMITTED TO
THE GRADUATE SCHOOL OF NATURAL AND APPLIED SCIENCES
OF
MIDDLE EAST TECHNICAL UNIVERSITY

BY

CEMRE KUŞOĞLU SARIKAYA

IN PARTIAL FULFILLMENT OF THE REQUIREMENTS
FOR
THE DEGREE OF MASTER OF SCIENCE
IN
PHYSICS

FEBRUARY 2011

Approval of the thesis:

OPTICALLY STIMULATED LUMINESCENCE STUDIES ON NATURAL FLUORITES

submitted by **CEMRE KUŞOĞLU SARIKAYA** in partial fulfillment of the requirements for the degree of **Master of Science in Physics Department, Middle East Technical University** by,

Prof. Dr. Canan Özgen
Dean, Graduate School of **Natural and Applied Sciences** _____

Prof. Dr. Sinan Bilikmen
Head of Department, **Physics** _____

Assoc. Prof. Dr. Enver Bulur
Supervisor, **Physics Dept., METU** _____

Examining Committee Members:

Prof. Dr. Güneş Tanır
Physics Dept., Gazi University _____

Assoc. Prof. Dr. Enver Bulur
Physics Dept., METU _____

Prof. Dr. Hamit Yurtseven
Physics Dept., METU _____

Prof. Dr. Nizami Hasanli
Physics Dept., METU _____

Assoc. Prof. Dr. Akif Esendemir
Physics Dept., METU _____

Date: 09/02/2011

I hereby declare that all information in this document has been obtained and presented in accordance with academic rules and ethical conduct. I also declare that, as required by these rules and conduct, I have fully cited and referenced all material and results that are not original to this work.

Name, Last name: CEMRE KUŞOĞLU SARIKAYA

Signature :

ABSTRACT

OPTICALLY STIMULATED LUMINESCENCE
STUDIES ON NATURAL FLUORITES

Kuşoğlu Sarıkaya, Cemre
M.Sc., Department of Physics
Supervisor: Assoc. Prof. Dr. Enver Bulur

February 2011, 90 pages

Optically Stimulated Luminescence (OSL) is the luminescence emitted from a previously irradiated insulator (or a wide band gap semiconductor) upon exposure to light. The OSL signal intensity is a function of the radiation dose absorbed by the sample and thus can be used as the basis of a radiation dosimetry method. In the literature, OSL studies on natural fluorites are rather limited. In order to promote the material for radiation dosimetry, OSL properties of natural fluorites of different origin were examined in this study. For this purpose, dose-response, reproducibility, thermal stability and fading of the OSL signals were analyzed. In order to find a relation between OSL and TL signals, TL signals and the effect of OSL measurements on TL signals were examined. Thermal activation energies of the light sensitive TL peaks and the OSL signals were also calculated using different methods and the results were compared. Also, absence of the thermal quenching was shown. Finally, TR-OSL signals were measured to have an opinion about the recombination centers. As a result of these studies, it is possible to conclude that natural fluorites show promising features to be used as an environmental dosimeter with regard to a suitable OSL signal, range of linearity, repeatability in response, as well as being readily available at a low cost.

Keywords: Luminescence Dosimetry, Natural Fluorites, Optically Stimulated Luminescence (OSL), Thermoluminescence (TL), Time-Resolved OSL (TR-OSL).

ÖZ

DOĞAL FLORİTLERDE OPTİK UYARMALI LÜMİNESANS ÇALIŞMALARI

Kuşoğlu Sarıkaya, Cemre
Yüksek Lisans, Fizik Bölümü
Tez Yöneticisi: Doç. Dr. Enver Bulur

Şubat 2011, 90 sayfa

Optik uyarmalı lüminesans (OSL), iyonlaştırıcı radyasyonla ışınlanmış katı (yalıtkan ya da geniş bant aralıklı yarı iletken) bir malzemenin ışığa maruz bırakılması sonucu lüminesans (ışık) yayması olayıdır. OSL sinyalinin şiddeti, numune tarafından soğurulan radyasyon dozuna bağlıdır ve bu bağımlılık radyasyon dozimetri yönteminin temelini oluşturur. Son zamanlarda doğal floritler ile ilgili OSL çalışmaları yapılmış olmasına rağmen malzeme, OSL tekniği ile çok detaylı olarak çalışılmamıştır. Bundan dolayı, bu çalışmada, farklı yerlerden temin edilen floritlerin OSL özellikleri incelendi. Bu amaçla, OSL sinyalinin doz-cevap eğrisi, tekrarlanabilirliliği, termal kararlılığı ve fading (solma) özelliği analiz edildi. OSL ve TL sinyalleri arasında bir ilişki bulabilmek amacıyla, TL sinyalleri ve OSL ölçümlerinin TL sinyalleri üzerindeki etkisi incelendi. Bunun yanısıra, OSL tuzaklarının termal aktivasyon enerjileri farklı metotlar ile hesaplandı ve sonuçlar karşılaştırıldı. Ayrıca, termal sönümlenme olayının olmadığı gösterildi. Son olarak, rekombinasyon merkezleri hakkında fikir edinebilmek için TR-OSL sinyalleri incelendi. Sonuç olarak, doğal floritlerin çevre dozimetresi olarak kullanılabilmesi için, ucuz elde edilebilir olmasının yanı sıra, uygun bir OSL sinyal yapısı, geniş lineer doz cevabı ve sinyalin tekrarlanabilirliliği açısından uygun OSL özelliklerine sahip olduğu gözlendi.

Anahtar Kelimeler: Doğal Floritler, Lüminesans Dozimetri, Optik Uyarmalı Lüminesans (OSL), Termolüminesans (TL), Zaman Tanımlı OSL (TR-OSL).

to my father…

ACKNOWLEDGEMENTS

I wish to express my deepest gratitude to my advisor, Assoc. Prof. Dr. Enver Bulur, for his encouragement, advice and guidance throughout this study.

I would also like to thank Prof. Dr. H. Yeter Göksu for her permission to use facilities of the Retrospective Dosimetry Laboratory in Institute of Nuclear Science at Ankara University.

I wish to thank The Scientific and Technological Research Council of Turkey (TÜBİTAK) for their financial support to my graduate study.

The hospitality and the help of Şule Kaya (Institute of Nuclear Science, Ankara University) are gratefully acknowledged.

I also want to thank Mahmut Emre Yağcı for his effort on programming of the TR-OSL system.

I am also grateful to my mother Mey and my father Reşad since they have not given up my hands up until now.

Finally, I want to thank my husband Onur for his understanding and support and for being in my life.

TABLE OF CONTENTS

LIST OF TABLES

TABLES

LIST OF FIGURES

FIGURES

CHAPTER 1

INTRODUCTION

Luminescence is the phenomenon which was not identified easily, although its different kinds were observed in many instances. In Greece, Aristotle (384-322 B.C.) observed light being emitted from decaying fish and wrote in his De Colóribus "Some things though they are not in their nature fire nor any species of fire, yet seem to produce light". Nearly two thousand years later in 1565, a Spaniard, Nicolas Monardes wrote about the unusually intense blue color of an aqueous extract of a wood which is called *lignum nephriticum (Mexican kidneywood)*. About ninety years afterwards, this solution was studied by Athanasius Kircher in Germany, Francesco Grimaldi in Italy, and Robert Boyle and Isaac Newton in England. All reported that when it was illuminated with white light, it appeared intensely blue by reflection, and yellow by transmission. None identified the intense blue light as luminescence emission. Later, the Englishman George Stokes made this identification by using optical filters and prisms. He showed that incident light of one spectral region was absorbed and transformed by the solution into emitted light of a different spectral region of longer wavelength. He also showed that this emission of luminescence stopped suddenly when the incident light was shut off, as did the emission from specimens of the mineral fluorspar. Therefore, Stokes decided to call these phenomena fluorescence, from fluorspar.

Bolognian Vincenzo Cascariolo observed luminescence from powdered natural barite (barium sulphate). He heated this sample with coal and found that the cooled porous cake glowed at night. This was the first observation reported about

luminescence of solids and it was reported in 1603. Cascariolo also found that this new "stone" apparently absorbed light from the sun by day, and then glowed for hours in the dark; for this reason it was called *lapis solaris (sun stone)*. Later, it came to the attention of Galileo Galilei. He got samples and gave them to Gulio Lagalla of the Collegio Romano. Lagalla wrote about lapis solaris and its extraordinary glow in De Phaenomenis in Orbe Lunae, 1612. Since the "stone" was porous, it was also called *spongia solis* (sun sponge) under the assumption that it simply absorbed and later released the light of the sun. In 1652, however, Nicolas Zucchi used optical filters to show that the color of the light given off at night was the same whether the "stone" was previously exposed to white light or light of other colors, such as blue or green. Meanwhile, in 1640, Fortunio Liceti wrote the first monograph on the Bolognian "stone", with the Greek title *Litheosphorus*, or "stony phosphorus", where phosphorus means light bearer. Since then, microcrystalline solid luminescent materials have come to be called phosphors to distinguish them from the chemical element phosphorus, which was isolated by Hennig Brand in 1669, and labelled phosphorus by Johann Elsholz in 1677. Because Cascariolo's original phosphor glowed long after excitation, long-persistent luminescence emission was called phosphorescence.

It was not until 1888 that the German physicist Eilhard Wiedemann introduced the term luminescence, of latin origin, to include both fluorescence and phosphorescence. Wiedemann defined luminescence as denoting "all those phenomena of light which are not caused solely by a rise in temperature". Today, luminescence is considered to be a process by which a material generates nonthermal radiation that is characteristic of the particular material. Luminescence is associated with defects (native or foreign) of solid structure.

As well as there are various luminescence emissions from different materials, there are different kinds of excitation source causing luminescence. One of them which was mostly used in this study is light. When the excitation is made by means of light,

the luminescence is called Photoluminescence (PL). However, the phenomenon used in this study is the Optically Stimulated Luminescence (OSL) which is also caused by excitation via light. The difference is hidden in the purpose. If light is used mainly for the purpose of determining the defect's structure by exciting the electron with photon from the defect's ground state to defect's excited state, then the arising luminescence is called Photoluminescence. OSL, however, is resulted in an irradiated insulator (or a wide band gap semiconductor) upon exposure to light. When the material is exposed to radiation, electron-hole pairs are created by ionization. Then, these pairs are trapped in pre-existing defects of the material. Absorption of photons causes the transition of the trapped electrons to conduction band. Recombination of these electrons with the trapped holes results in radiative emission which is called OSL. There is also another luminescence type which is called Thermoluminescence (TL). It has the same process as OSL but the stimulation of the material is done by heating, not by photons. As inferred from the definitions, OSL and TL intensities are functions of absorbed radiation. Hence, these two luminescence types are used mostly in dosimetric applications. Further details about OSL and TL mechanisms will be given in Chapter 3.

OSL was first suggested by Antonov-Romanovskii et al. (1956) for a radiation dosimetry application and was later used by Bräunlich et al. (1967) and Sanborn and Beard (1967). In spite of these early developments, OSL had not been used extensively in radiation dosimetry because of the lack of a good luminescent material, which is highly sensitive to radiation, and have a high optical stimulation efficiency, a low effective atomic number and good fading characteristics (i.e., a stable luminescence signal at room temperature). MgS, CaS, SrS and SrSe doped with different rare earth elements such as Ce, Sm and Eu were among the first phosphors suggested for OSL dosimetry applications (Bräunlich et al., 1967; Sanborn and Beard, 1967; Rao et al., 1984). They showed a high sensitivity to radiation and a high efficiency under infra-red stimulation at a wavelength around 1 μm. However, as well as they have a very high effective atomic number which is not suitable for use in personal dosimetry, they also show significant fading of the

luminescence at room temperature. By the usage of filtered lamps and light emitting diodes as stimulation sources and the observation of good OSL dosimetric characteristics of Al_2O_3:C samples in 1995 (Markey et al., 1995), OSL became an important method in dosimetric applications. Al_2O_3:C is virtually the only synthetic dosemeter used in medical, environmental, and personnel dosimetry (Bøtter-Jensen et al., 2003). Latest developments about the OSL dosimetry have been described in proceedings of the 15th solid state dosimetry (SSD15) (Bos, 2008).

OSL has become a popular method in age determination of archeological and geological findings. In this application, dose of radiation absorbed by the mineral since it was last exposed to light is determined by integrating the OSL signal and then calibrating it against known doses of radiation. The age is obtained by taking into account also the environmental dose rate. Huntley et al. (1985) first used OSL for this purpose and the latest developments in this field can be found in the proceedings of triennial conferences on luminescence and ESR dating (LED) (McKeever, 2000, 2003; Bailiff and Wintle, 2006; Bailiff et al., 2009).

In this study, OSL properties of natural fluorites were investigated with the aim of checking the possibility of using the material for environmental dosimetry. Fluorite (CaF_2), known as fluorspar commercially, is the mineral which can form in different geological environment as crystalline blocks. It consists of % 51.1 calcium and % 48.9 fluorine when it is pure. The natural fluorite can be found with quartz, barite, calcite, galena, sphalerite, siderite, celestite, chalcopyrite and other sulfide minerals. This mineral is among the most colorful ones. As well as it can be colorless, it can have violet, blue, yellow, green, pink, red, brown colors according to impurities, exposed radiation and size of the color centers. In Turkey, fluorites are found in Kırşehir, Yozgat and Eskişehir. Among these, the quality of Kırşehir (Çicekdağı, Akçakent and Kaman parts) fluorites is acceptible to the world specifications (DPT: 2618 – ÖİK: 629).

In terms of dosimetric properties, CaF_2 is a well-known TL material and it is among the earliest mineral used for this purpose. It can be used as a dosimeter both in natural or in synthetic forms. High TL intensity and its low cost make the natural fluorite an important material for TL dosimetry. Similarly, synthetic fluorite is also very popular because of its enhanced sensitivity and its simple glow curve structure depending on the dopant (McKeever et al., 1995). These advantages indicated that this material can be a good environmental dosimeter (McKeever et al., 1995). However, it can not be used in personal dosimetry applications since it is not tissue equivalent (McKeever et al., 1995; Bos 2001). The TL properties of fluorite in both natural and synthetic form have been extensively reported (Nambi 1975; Sunta 1984; Urbina et al., 1998; Balogun et al. 1999; Sohrabi et al., 1999; Topaksu and Yazıcı, 2007). Nevertheless, there are few OSL studies reported on natural fluorites (Chougaonkar and Bhatt, 2004; Polymeris et al., 2006; Yoshimura and Yukihara, 2006) although it was reported to be very sensitive to light independent of the dopant used (McKeever et al., 1995; Calderon et al., 1990). Chougaonkar and Bhatt (2004) have investigated the OSL signal and the Linearly Modulated OSL (LM-OSL) signal of natural fluorites and they have related these signals with the TL peaks observed. Later, Polymeris et al. (2006) have investigated the OSL sensitivity and the lowest detectable dose limit (LDDL) of natural fluorite and they have also tried to find a relation between its OSL components and individual TL glow peaks. Among these recently reported studies, some of the OSL properties of natural fluorites have also been investigated by Yoshimura and Yukihara (2006). As well as the dosimetric properties of this mineral obtained from the reported studies mentioned above, the structural and optical characteristics of natural fluorites will also be discussed in detail in Chapter 4.

In light of the foregoing, the OSL properties of the natural fluorites of different origins have been discussed in this study. For this purpose, several experiments which will be mentioned in Chapter 6 were performed. According to the findings, the usability of this mineral as an OSL dosimeter in environmental dosimetry applications will be discussed in Chapter 7.

CHAPTER 2

POINT DEFECTS

There is no solid without any defect, which is called perfect solid, in nature because of the second law of thermodynamics. This law states that zero entropy is only possible at absolute zero temperature. Therefore, all solids that we are dealing with have some defects which bring in these solids special features.

In a three-dimensional solid, three major types of defects, one-, two- and three-dimensional, exist. They are called point, line (edge) and volume (plane), respectively. Point defects are the changes at atomistic levels and they can come into existence as a result of absence of an atom, substitution in a lattice or settling in lattice interstices (Fig. 2.1). They affect the physical and chemical properties of the solid. Nevertheless, line and volume defects are the changes at molecular levels. The former is caused by lack of ordering along the plane and the latter is generated from the interior to the surface of the crystal because of propagation of the line defects to the surface where the actual crystal growth takes place. As it appears, they affect only the physical properties of the solid. Despite all of these effects, the structure of the solid does not change in the presence of defects.

Point defects vary with solid type, i.e. heterogenous or homogenous solid. Types of point defects expected in a homogenous solid (Fig. 2.1):

a) Vacancies

b) Self-interstitial
c) Substitutional impurities
d) Interstitial impurities

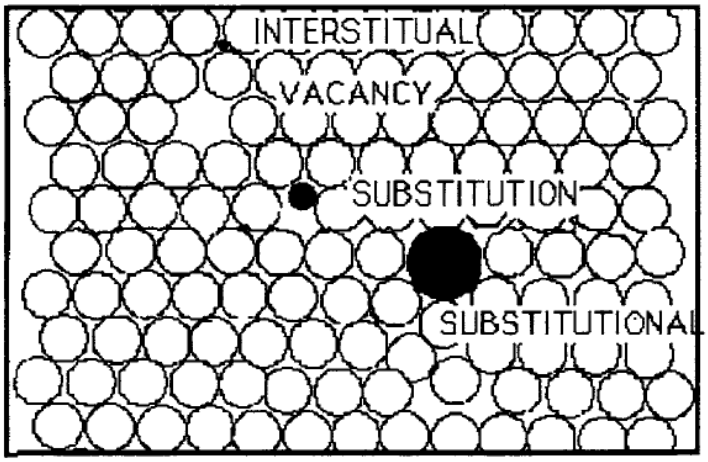

Figure 2.1 Point defects in the hexagonally-close packed lattice (After, Ropp, 2004).

However, types of point defects expected in a heterogenous solid are limited because of charge compensation mechanism and the presence of two sub-lattices in an ionic solid. They can be listed as following.

a) Schottky defects (absence of cation and anion)
b) Cation vacancies
c) Anion vacancies
d) Frenkel defects (cation vacancy plus same cation as interstitial)
e) Interstitial impurity atoms (both cation and anion)
f) Substitutional impurity atoms (both cation and anion)

These defects are demonstrated in Fig. 2.2. Furthermore, there is anti-Frenkel defects which can exist in the anion sub-lattice. Other than these defects, there are also charged vacancies. However, negatively charged cation vacancy and positively charged anion vacancy would not be very stable. Because the first one would be

surrounded by anions and the other one would be surrounded by cations. Hence, the possible stable charged vacancies are negatively charged anion vacancy and positively charged cation vacancy. Especially, negatively charged vacancy is called *F*-center (from the German word Farbe meaning color) provided that it is optically active. This center occurs when an electron captured in an anion vacancy because of charge-compensation. It is also called color-center as it imparts a specific color to the crystal. More than one color center in a crystal are also possible. In such a case, for instance, when there are two anion sites, they can join to form the *M*-center.

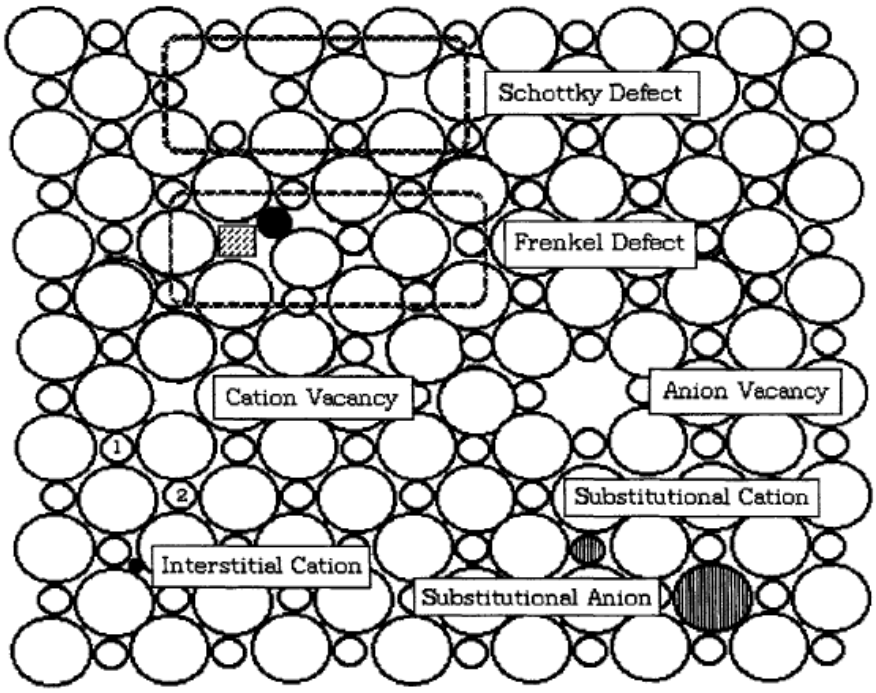

Figure 2.2 Point defects which can occur in the heterogeneous ionic solid having hexagonal lattice structure (After, Ropp, 2004).

Point defects are used in broad variety of commercial products. These include transistors, integrated circuits, photosensors, color-television, fluorescent lamps. None of these would be possible without point defects. In addition, these defects are of basic importance in dating and dosimetry applications. Because they store the electrons and this property is the basis of these applications. The reason will be

understood after the discussion of following chapter. Therefore, this chapter is devoted to point defects.

CHAPTER 3

LUMINESCENCE

The emission of light is always resulted from an input of energy of some type. Therefore, luminescence, which is also called the cold light phenomenon, is defined as the emission of non-thermal radiation by a molecule, solid or an atom after absorption of energy as it is shown in Fig. 3.1.

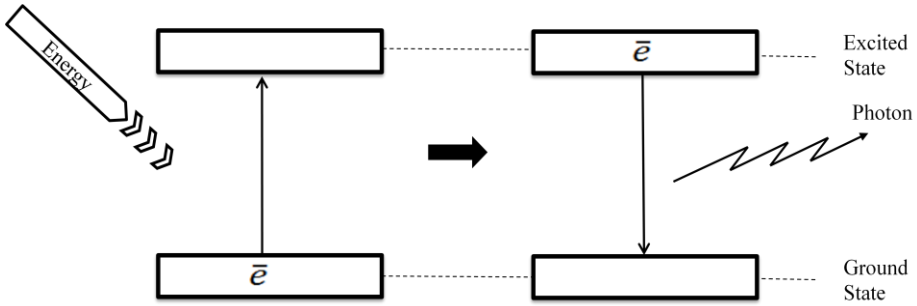

Figure 3.1 General representation of luminescence phenomenon.

The time required for absorption of photon or transition of an electron to an excited state is ~10^{-15} s. Furthermore, Franck-Condon principle assumes that electronic transitions are vertical. This means that after electronic transitions take place, nuclear position does not change since electronic transitions occur faster than nuclear motion because of huge difference between masses of an electron and a nucleon. Representation of luminescence transition according to this principle is shown in Fig. 3.2.

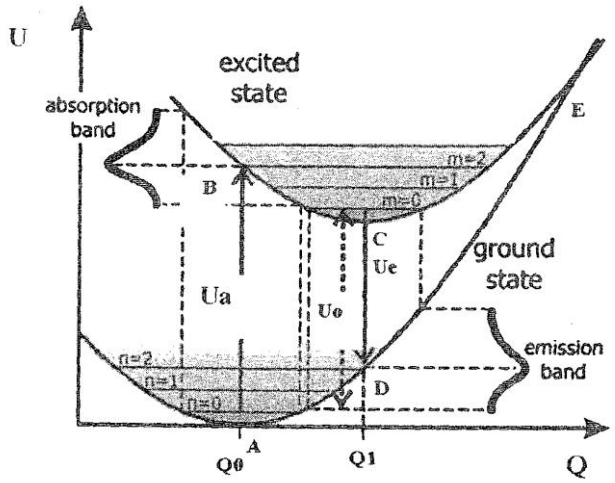

Figure 3.2 General scheme for explanation of luminescence transition according to the Franck-Condon principle in a configurational coordinate diagram, showing the parameters energy (U) and configurational coordinate (Q). The excitation from the vibrational level n=0 of the ground state to the excited state result in an absorption band with the energy U_a. The relaxation of the system, i.e. from vibrational level m=0 of the excited state to the ground state, causes an emission band with the energy U_e. The energy difference between the lowest possible vibrational levels of the ground and excited state (n=0 and m=0) is U_0, with $U_a > U_0 > U_e$ (After, Gaft et al., 2005).

There are various types of excitation mechanisms cause different kinds of luminescence. These excitation sources and the name of the emissions resulted by these excitations are listed in Table 3.1.

Among different forms of luminescence, the most important one from the point of view of this study is the photoluminescence (PL). It is used mainly to obtain an information about defects of the material via exciting the electron with photon from defect's ground state to defect's excited state. Relaxation back to the ground state results in the emission of light the intensity of which is proportional to the

concentration of excited defects. PL can be seen in two different forms which are called fluorescence and phosphorescence. These will be revealed in detail in the following sections.

Table 3.1 Luminescence types caused by different excitation sources.

Luminescence Type	**Excitation Source**
Photoluminescence	Photons
Radioluminescence	Particles emitted from radioactive materials
Chemiluminescence	Particles produced in chemical reactions
Röntgenoluminescence	X rays
Electroluminescence	Electrons
Mechanoluminescence	Any mechanical action on a solid
Thermoluminescence	Heating
Ionoluminescence	Positive or negative ions
Sonoluminescence	Sound
Crystalloluminescence	Produced during crystallization

3.1 Fluorescence and Phosphorescence

As it appears from the definition of PL, it is caused by emission of light after absorption of light. These emission and absorption mechanisms are resulted by electronic transitions between the energy levels. Hence, it is important to know about the electronic states to discuss about fluorescence and phosphorescence processes.

3.1.1 Electronic States

There are mainly two significant states, important for the fluorescence and phosphorescence; singlet states and triplet states. Furthermore, each of these states

have vibrational levels superimposed on them. The vibrational levels are induced as a result of an excess energy arising from lattice vibrations. It is assumed that molecules are in the lowest vibrational level of the ground state at room temperature.

According to Pauli exclusion principle, two electrons with the same quantum numbers can not occupy the same quantum state. That is to say, only if two electrons have their spins paired, they can occupy the same orbital. When all of the electrons in a molecule are spin paired, as seen in Fig. 3.3, the state is called a singlet state. Because of spin pairing, there is no net spin angular momentum and thus this state is diamagnetic which means that it is neither attracted nor repelled by a static magnetic field. However, if one set of electron spins is unpaired, as shown in Fig. 3.3, then the state is called a triplet state. This state is so called because it splits up into three sub-states in existence of magnetic field because it has an overall spin angular momentum. Therefore, it is paramagnetic.

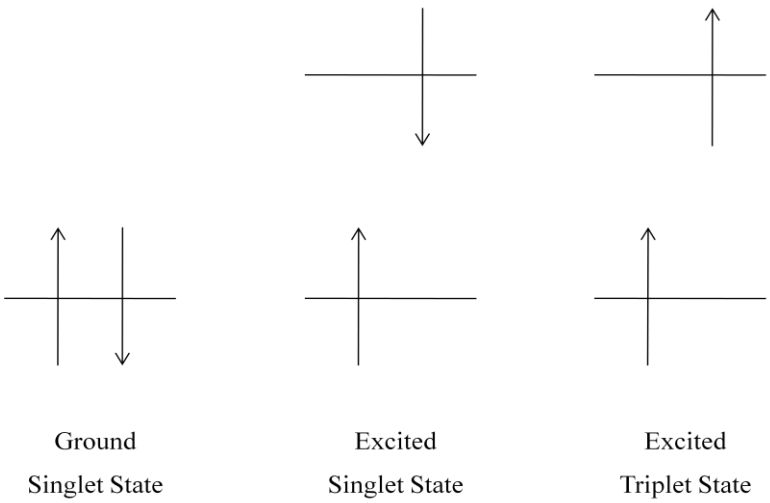

Figure 3.3 Electronic states; Singlet and Triplet state.

It should be noted that for every excited singlet state, there is a corresponding excited triplet state and excited triplet state always has a lower energy because of spin

direction of unpaired electron. Also, the transition from ground state into triplet states and the transitions between triplet and singlet states are forbidden because of the selection rule $\Delta S = 0$, where S is the total spin quantum number.

3.1.2 Fluorescence

After absorption of a photon (visible or UV), an electron makes transition to the excited singlet state and then make a radiationless transition to the zeroth vibrational level of this state. If electrons return to the ground state with emission of light, this phenomenon is called fluorescence and it is described schematically in Fig. 3.4. The lifetime of the excited singlet state is approximately 10^{-8} s. So, the Fluorescence occurs within the same period of time. As it appears from the Fig. 3.4, the wavelength of the emitted light is greater than that of the absorbed light because of radiationless transitions between the vibrational levels of an excited state and that of a ground state. This shift in wavelength is called Stokes' shift.

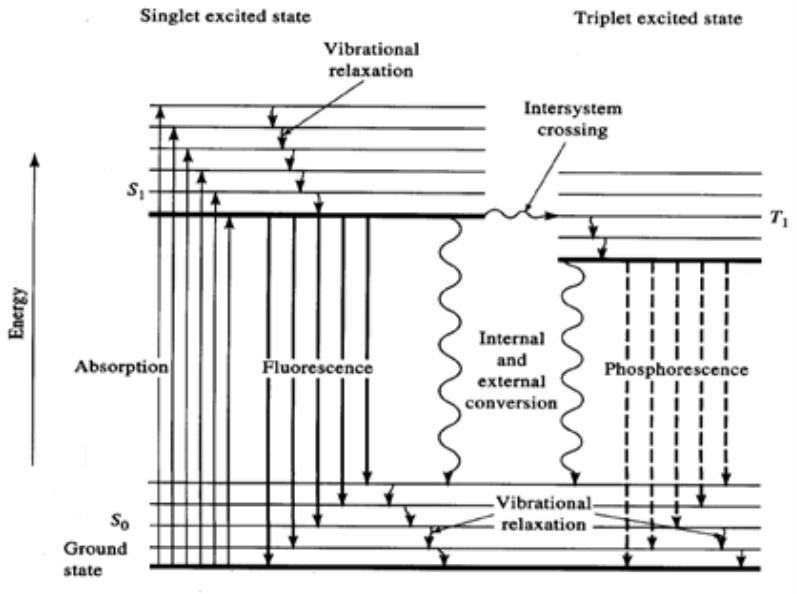

Figure 3.4 Partial energy diagram for a photoluminescent system (Redrawn after, Skoog D. A. et al., 1998).

By means of the equipments used for fluorescence spectroscopy, one can observe either an excitation spectrum or an emission spectrum for an investigated material. Excitation spectrum is obtained by changing the wavelength of excitation light and plotting the fluorescence emission intensity versus wavelength of this light. This spectrum is also known as fluorescence absorption spectrum. On the contrary, emission spectrum is obtained by exciting the material with light having an energy which is maximum absorbed and then by scanning the fluorescence emission with a monochromator. Hence, the graph is the fluorescence emission intensity versus emission wavelength which is named as emission spectrum.

3.1.3 Phosphorescence

Phosphorescence is the light emission as a result of intersystem crossing. Actually, the transition from a singlet state to a triplet state is forbidden because of the selection rule $\Delta S = 0$, where S is the total spin quantum number. However, spin-orbit coupling effect makes this transition weakly possible. Therefore, after absorption of photon or transition of the electron to an excited singlet state, transition from the lowest excited singlet state to an excited triplet state occurs. This transition is called as intersystem crossing and its life time is the same as that of the excited singlet state which is approximately 10^{-8} s. Then, radiationless relaxation to zeroth vibrational level of the excited triplet state happens. If turning of an electron from this level to ground state results in emission of light, this phenomena is called phosphorescence and it is a slow process with lifetime ranging between 10^{-4} to 10 s relative to fluorescence process owing to long life time of triplet state.

As mentioned before, the energy of the excited triplet state is always lower than that of excited singlet state. For that reason, phosphorescence occurs at a lower energy

than fluorescence. Thereby, the Stokes' shift is also observed for the phosphorescence mechanism.

3.2 Optically Stimulated Luminescence

Optically stimulated luminescence (OSL) -also called Photo-Stimulated Luminescence (PSL)- is a kind of PL. But, it has some different processes. OSL is the emission of light from an irradiated semiconductor (wide band-gap) or insulator during optical stimulation. Irradiation with ionizing radiation creates free electrons and holes in the material. Then, part of these electron-hole pairs can be captured by defects of the material which are called traps. These traps are deep enough to accumulate charges. After the storage period, stimulation with light gives rise to transition of the trapped electrons to the conduction band. As a result, emission of luminescence occurs after recombination of these electrons with optically active trapped holes which are also named as recombination centers. This explanation of OSL process is embodied in Fig. 3.5. By reason of this process, OSL decay curve, the OSL emission plotted as a function of time, is observed (Fig. 3.6). As shown, OSL emission is monotonically decreased as a function of time because electron population in the traps is limited. The shape of this decay is dependent upon the sample, the absorbed dose, the illumination intensity and the temperature.

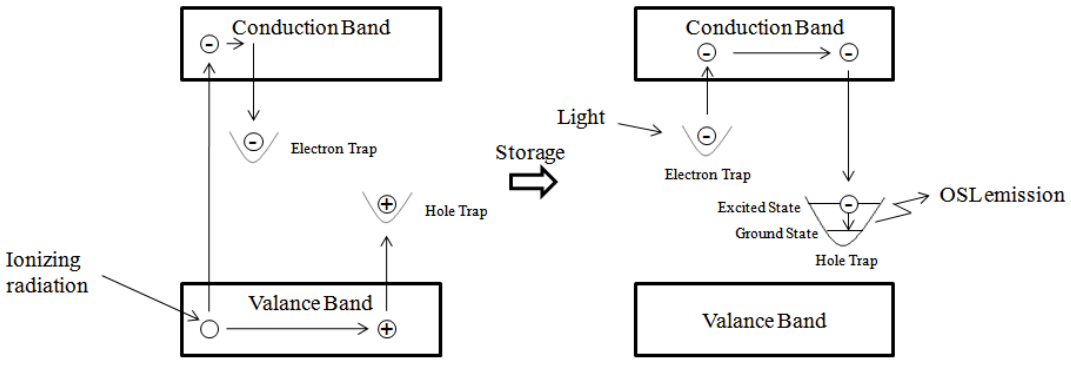

Figure 3.5 The OSL process.

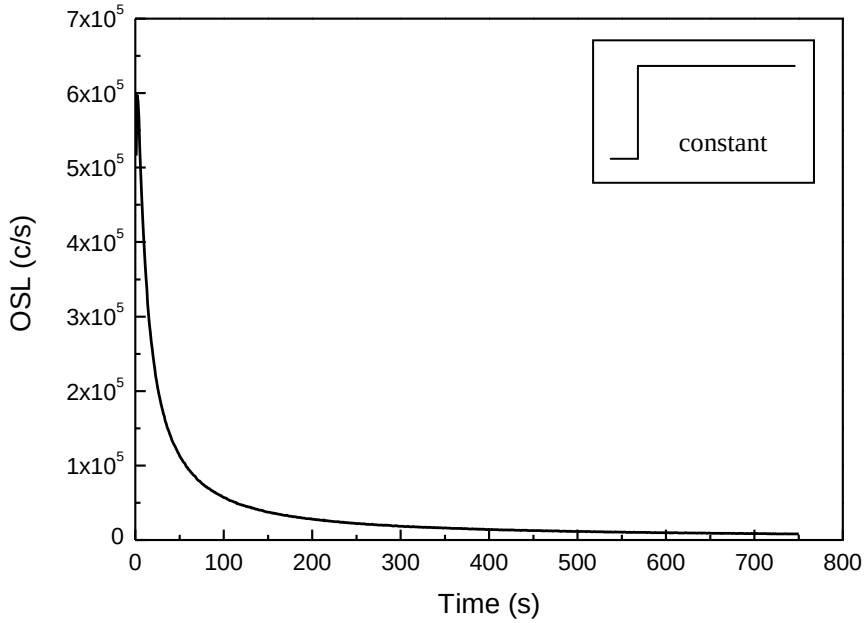

Figure 3.6 A typical OSL decay curve. Inset to graph represents the stimulation light intensity against time.

It should be noted that, the wavelength of the emitted light is shorter than that of stimulation light in OSL mechanism. Although, this shift seems like Anti-Stoke's shift, it is not because of electron storage process.

Because the electron population in the traps is dependent on the absorbed dose, the OSL intensity is the function of the dose of radiation absorbed by the material. This makes the technique suitable for radiation dosimetry.

3.2.1 OSL Stimulation Modes

Optically Stimulation can be done in three ways according to purpose of investigation;

a) Stimulation light intensity can be kept constant (Continuous-Wave OSL).
b) Stimulation light intensity can be ramped linearly (Linearly Modulated OSL).
c) Stimulation source can be pulsed and the OSL can be measured between the pulses (Pulsed OSL).

3.2.1.1 Continuous-Wave OSL

In Continuous-Wave OSL (CW-OSL) the stimulation light intensity is kept constant throughout the measurement. Hence, the discrimination of the stimulation light and the emitted light is required. This is achieved by using the combination of suitable optical stimulation and detection filters. So, as it appears, the OSL traps which have certain energies can be investigated and the emission can be observed in a specific wavelength range in this stimulation mode. The shape of the OSL signal obtained from this method was given in Fig. 3.6.

There are two main OSL stimulation types with respect to wavelength of the stimulation light: Infrared stimulated luminescence (IRSL) and Visible light stimulated luminescence.

3.2.1.2. Linearly Modulated OSL

Because of the constant stimulation light intensity, general picture of traps having various photoionization cross-section which is the probability of interaction of trapped electrons with a photon can be obtained from CW-OSL method. Whereupon, Bulur (1996) introduced a new method to observe these traps separately. This method is called Linearly Modulated OSL (LM-OSL). Here, OSL is monitored while the intensity of the stimulation source is ramped linearly. As a result of this measurement, OSL signal is seen as a series of peaks which point out to the optical release of charge from different trap types as it is seen in Fig. 3.7.

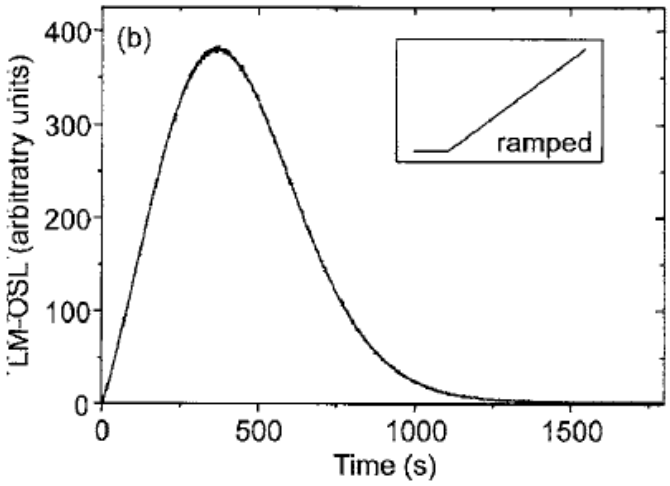

Figure 3.7 A typical LM-OSL signal. Inset to graph represents the intensity (After, Bøtter-Jensen L. et al, 2003).

3.2.1.3 Pulsed OSL

Another modification, Pulsed OSL (POSL) was used by McKeever, Akselrod and colleagues (Markey et al., 1995; McKeever et al., 1996; Akselrod and McKeever,

1999) using crystalline Al_2O_3:C as the luminescent material. In this method, stimulation source is pulsed and OSL is monitored only after the end of the pulse. This technique enables us to separate the recombination centers which have different lifetimes.

Since less optical filtration is required than with CW-OSL, the emission light can be observed in a broader wavelength range. Furthermore, as well as very rapid OSL measurement is possible because of short pulses given to the sample, multiple readout of one sample is also feasible as the signal is not depleted in one reading. An example of POSL signal is illustrated in Fig. 3.8.

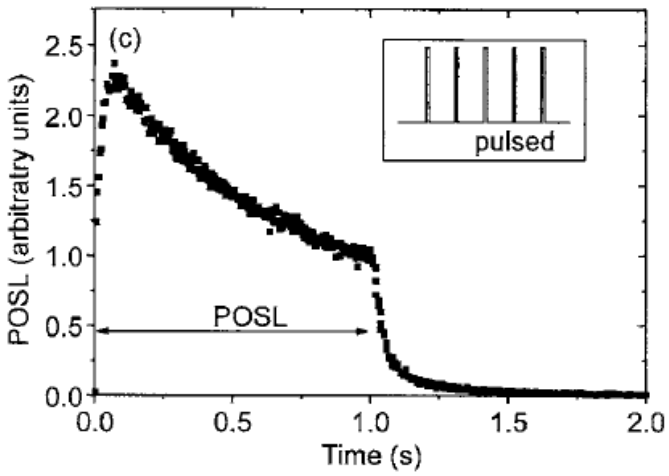

Figure 3.8 A typical POSL signal. Inset to graph represents the intensity (After, Bøtter-Jensen et al., 2003).

3.2.2 Models and Rate Equations

The OSL process can be explained mathematically by a series of non-linear, coupled rate equations which are intractable. To reach an analytical expression for the

evolution of the OSL intensity with time during optical stimulation and, ultimately, for the dependence of the OSL signal on the absorbed dose, several simplifying assumptions are required. Thence, some models which were introduced before to understand a solid structure are used for applying them to experimental results to understand the OSL properties of the sample investigated. Each of them includes transport of electrons through the conduction band in order for them to reach the trapped holes which are the radiative recombination centers. Among these models, the simplest one is the one- trap/one-center model which is shown in Fig. 3.9.

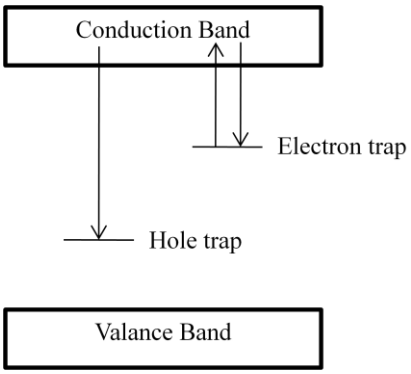

Figure 3.9 The one-trap/one-center model.

This model includes one type of electron trap and one type of hole trap. After the electrons are excited with the rate of stimulation p (in units of s^{-1}) from the traps to the conduction band, they either recombine with the trapped holes and OSL emission occurs or they are re-trapped. To describe this phenomena mathematically, first of all charge neutrality for this system should be written as:

$$n_c + n = m_v + m \tag{3.1}$$

where n_c and n are the concentrations of electrons in the conduction band and the traps, respectively, and m_v and m are the concentrations of holes in the valance band and hole traps, respectively.

During optical stimulation of the electrons from the traps, transitions to the valance band do not occur. Hence, the charge neutrality condition becomes $n_c + n = m$. Then, the rate of change of the various concentrations can be written as:

$$\frac{dn_c}{dt} = -\frac{dn}{dt} + \frac{dm}{dt} \tag{3.2}$$

The terms on the right-hand side may be written explicitly as:

$$\frac{dn}{dt} = -np + n_c A(N - n) \tag{3.3}$$

and

$$\frac{dm}{dt} = -n_c A_m m = -\frac{n_c}{\tau} \tag{3.4}$$

Here, p is a positive function of the incident photon flux ϕ and the photoionization cross-section σ for the monochromatic light.

$$p = \sigma\phi \tag{3.5}$$

The other terms in Eqs. (3.3) and (3.4) include A, the retrapping probability (in units of $m^3 s^{-1}$); A_m, the recombination probability (also in units of $m^3 s^{-1}$); N, the total available concentration of electron traps (in m^{-3}); and $\tau = 1/A_m m$, the free electron recombination lifetime (in s). With the assumptions of quasi-equilibrium ($dn_c/dt \ll dn/dt, dm/dt$ and $n_c \ll n, m$) and negligible re-trapping ($n_c A(N - n) \ll np, n_c A_m m$) we have

$$I_{OSL} = -\frac{dm}{dt} = -\frac{dn}{dt} = np \tag{3.6}$$

the solution of which is

$$I_{OSL} = n_0 p \exp(-tp) = I_0 \exp(-t/\tau_d) \tag{3.7}$$

Here, n_0 is the concentration of trapped electrons at time t=0, I_0 is the luminescence intensity at t=0, and $\tau_d = 1/p$ is the decay constant. It is deduced from this equation that according to the simplest model, OSL decay curve has a simple exponential form and in the end, OSL becomes zero since all the traps are depleted (McKeever et al., 1997a). However, the experimental OSL decay curves generally do not conform to this simple exponential form. Because these curves may involve significant re-trapping process or different trap types which have different photo-ionization cross-sections. Therefore, Chen and McKeever (1997) have showed that in case of significant re-trapping, the OSL intensity is written as:

$$I_{OSL} = np - n_c A(N - n) \tag{3.8}$$

For the specific case of $N \gg n$, and $R = A/A_m \gg n/(N - n)$, a second-order function results, namely:

$$I_{OSL} = \frac{n^2 p}{NR} = -\frac{dn}{dt} \tag{3.9}$$

The solution, after integration, is:

$$I_{OSL} = I_0 \left(1 + \frac{n_0 pt}{NR}\right)^{-2} \tag{3.10}$$

where $I_0 = n_0^2 p/NR$. For the more general case of $I_0 = n_0^b p/NR$ we have:

$$\left(\frac{I_{OSL}}{I_0}\right)^{\frac{1-b}{b}} = \left(1 + \frac{n_0 pt}{NR}\right) \tag{3.11}$$

or

$$I_{OSL} = I_0 \left(1 + \frac{n_0 pt}{NR}\right)^{\frac{b}{1-b}} \tag{3.12}$$

If there are two optically active traps (concentrations n_1 and n_2 and stimulation rates p_1 and p_2), it is straightforward to show that (McKeever et al., 1997a,b):

$$\frac{dm}{dt} = -\frac{dn_1}{dt} - \frac{dn_2}{dt} \tag{3.13}$$

and that

$$\begin{aligned} I_{OSL} &= n_{10} p_1 \exp\left(-tp_1\right) + n_{20} p_2 \exp\left(-tp_2\right) \\ &= I_{10} \exp\left(-t/\tau_{d1}\right) + I_{20} \exp\left(-t/\tau_{d2}\right) \end{aligned} \tag{3.14}$$

using the superposition principle and no interaction between the traps. This equation can also be extended to three or more optically active traps, each emptying at their own characteristic rate during stimulation.

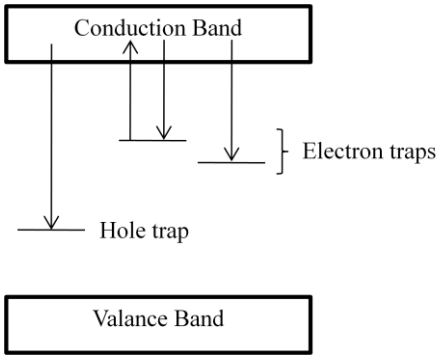

Figure 3.10 Model containing two electron traps one of which is optically inactive, and a hole trap.

Even the second trap which is the deep one is optically inactive as seen in Fig. 3.10, it affects the OSL intensity and in such a case, the intensity is described by:

$$I_{OSL} = n_{10} p \exp\left(-t/\tau\right) - \frac{dn_2}{dt} \tag{3.15}$$

where

$$\frac{dn_2}{dt} = n_c(N_2 - n_2)A_2 \tag{3.16}$$

In this equation, N_2, n_2 and A_2 are the concentration of available traps, concentration of filled traps, and trapping probability, respectively, for the deep trap. As shown from the equation, OSL intensity is reduced because of this additional deep trap and the decay is no longer exponential.

If the competing trap is shallow trap which is thermally meta-stable at the temperature of the OSL measurement, Eq. (3.17) becomes,

$$\frac{dn_2}{dt} = n_c(N_2 - n_2)A_2 - n_2 f \tag{3.17}$$

where f is the rate of thermal excitation out of the trap and it is described mathematically by the Arrhenius equation:

$$f(T) = s\exp\ -E/kT \tag{3.18}$$

where s and E are the frequency factor and thermal trap depth for the shallow trap and k is the Boltzmann's constant. Now we have for the OSL intensity:

$$I_{OSL} = n_{10}p\exp\ -t/\tau_d\ + n_2 s\exp\ -E/kT\ - n_c(N_2 - n_2)A_2 \tag{3.19}$$

The last two terms in Eq. (3.19) combine to produce a long-lived, temperature-dependent component to the OSL decay curve. The form of this component is an initial increase, followed by a decrease at longer times. Depending upon the relative size of this component compared with the first term, the overall OSL decay curve may exhibit an initial increase, followed by a decrease. The relative size of the two components also depends on the excitation rate p such that at low values of p, the temperature-dependent term may be significant.

In addition to these models, there is also another one which contains two recombination centers one of which is radiative and the other is non-radiative as shown in Fig. 3.11.

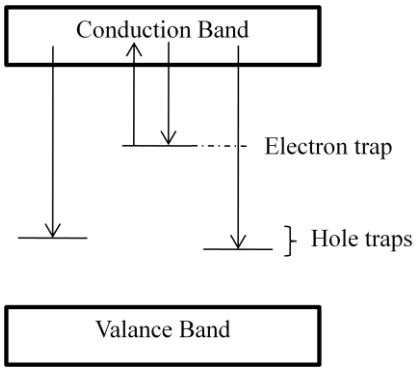

Figure 3.11 Model containing an electron trap and two recombination centers one of which is non-radiative.

In such a case the total trapped electron concentration n after irradiation is given by:

$$n = m_1 + m_2 \tag{3.20}$$

Here, m_1 and m_2 are the concentrations of trapped holes in the two recombination centers, respectively. Under these conditions, the OSL intensity is written as:

$$I_{OSL} = np \exp\left(-t/\tau_d\right) \left(-\frac{dm_2}{dt}\right) \tag{3.21}$$

Again, it is conceived from this equation that the intensity is reduced by the presence of a non-radiative recombination center as is the case in an additional optically inactive, deep electron trap. Quasi-equilibrium ($dn_c/dt \approx 0$) leads to:

$$m_1 = m_{10} \exp\left(-tn_c A_{m1}\right) \tag{3.22}$$

and

$$m_2 = m_{20} \exp\ -tn_c A_{m2} \tag{3.23}$$

where A_{m1} and A_{m2} are the recombination probabilities at the two centers, respectively. The relative size of the recombination centers is time-dependent, thus:

$$\frac{m_1}{m_2} \approx \frac{m_{01}}{m_{02}} \exp\ -tn_c\ \ A_{m1} - A_{m2} \tag{3.24}$$

In the circumstance that $A_{m1} \approx A_{m2}$, the ratio remains approximately constant. In this case, the OSL decay curve remains approximately exponential according to:

$$I_{OSL} = \frac{1}{K} n_0 p \exp\ -tp \tag{3.25}$$

where K is a constant given by $K = (m_1 + m_2)/m_1$. If the Eq. (3.25) is compared with the Eq. (3.7), it is observed that, as expected, the former case gives a weaker OSL signal (by a factor $1/K$).

The models revealed up to now are for very special cases only. Because real materials can contain all of the electron trap and recombination center types together. Therefore, the OSL decay curves obtained for these materials are much more complex. However, this difficulty can be surmounted by interpreting the experimental results in light of the basic information obtained from these models.

3.3 Thermoluminescence

Thermoluminescence (TL) has been used extensively to measure nuclear radiation doses since the early 1950s (Daniels et al., 1953), following the commercial availability of sufficiently sensitive and reliable photomultiplier (PM) tubes. As mentioned before, TL emission occurs as a result of the same process as that of OSL

except that electrons are stimulated from the traps by heating the sample at a constant rate. Consequently, a plot of TL signal as a function of temperature which is called glow curve is obtained as shown in Fig. 3.12. This signal may consist of several peaks occurring at different temperatures which relate to the different electron trap depths. Also, one peak may contain a number of overlapping peaks.

If the TL intensity is tried to be described mathematically, the rate equations which are the Eq. (3.2), Eq. (3.3), Eq. (3.4) are obtained except that the rate of the thermal excitation of the electrons from the traps at temperature T is given by Eq. (3.18) (instead of p). With the help of the quasi-equilibrium approximation and since the intensity of the TL emission is given by $I(T)=\eta n_c/\tau_t$, where η is the luminescence efficiency and τ_t is the thermal lifetime, then:

$$I(T)=\frac{\eta ns\exp\ -E/kT}{\left[\ 1/\tau_t\ +\ N-n\ \ A\right]} \tag{3.26}$$

With the inclusion of the slow retrapping or first order assumption we have, after integration:

$$I(T)=\eta n_0 s\exp\left(-\frac{E}{kT}\right)\exp\left[-\frac{s}{\beta}\int_{T_0}^{T}\exp\left(-\frac{E}{k\theta}\right)d\theta\right] \tag{3.27}$$

which is the Randall and Wilkins expression (1945) for TL with β is the heating rate, where $T=T_0+\beta t$. θ is a dummy variable representing temperature.

The TL curves exhibiting first-order kinetics are observed for some of the dosimetric materials. Therefore, the equations for non-first-order TL peaks will not be developed here. One can refer to books by Chen and Kirsh (1981) and by McKeever (1985) for further details.

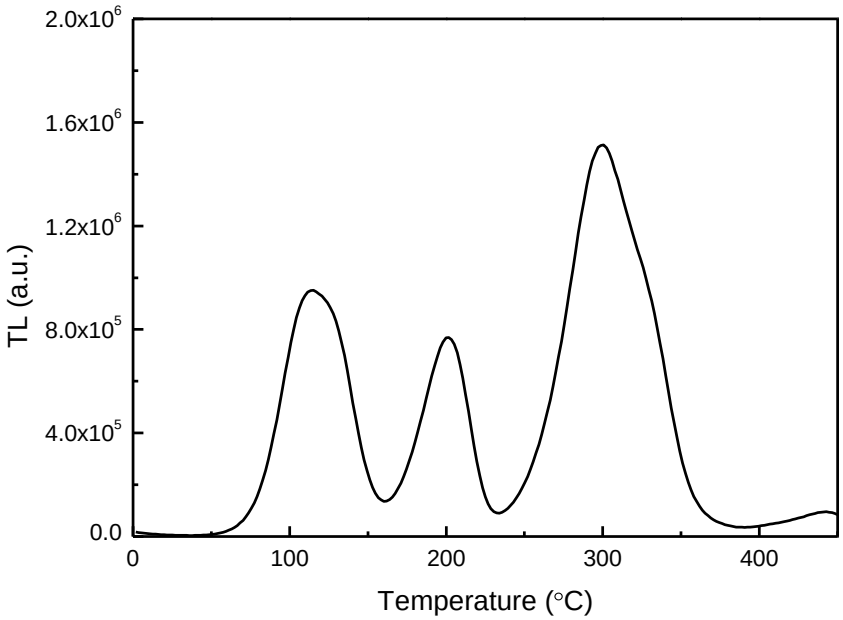

Figure 3.12 A typical TL glow curve.

The thermal lifetime of electrons in deep traps is longer than that of electrons in shallow traps. For that reason, traps observed at lower than 200 °C are not useful for dosimetric applications as the electrons in these traps can be stimulated even at environmental temperatures. However, anomalous fading of high temperature glow peaks at room temperature has been observed in some feldspars. This is result of quantum mechanical tunneling effect (Wintle, 1973). Another encountered problem in TL is thermal quenching. Thermal quenching is a reduction in the efficiency of luminescence as the temperature of the sample increases due to the opening up of competing, non-radiative relaxation pathways. For the detailed explanation of this phenomenon, one may refer to book by Bøtter-Jensen et al. (2003). Some high temperature peaks in quartz and feldspars are subject to this process (Wintle, 1975).

3.4 Time-Resolved OSL

Time-resolved optically stimulated luminescence (TR-OSL), which is also called POSL, is an alternative method for measurement of OSL. It deals with the recombination region of the OSL process. The technique was introduced by Sanderson and Clark (1994) who used an N_2 laser-based system to make exploratory measurements on alkali feldspars. Then, it has been used to study luminescence recombination processes in feldspar (Clark and Bailiff, 1998; Chithambo and Galloway, 2000; Tsukamoto et al., 2006; Denby et al., 2006), to assess the size of absorbed dose in dosimetry quality aluminium oxide (Markey et al., 1995; Akselrod and McKeever, 1999) and to investigate the properties of luminescence lifetimes in quartz (Bailiff, 2000; Galloway, 2002; Chithambo, 2003) and in calcite (Galloway, 2003)

In TR-OSL technique, sample is stimulated using a brief light pulse. During stimulation, the signal measured consists of a monotonically increasing luminescence component and constant scatter from the stimulating light which is described mathematically as $I(t) \propto 1-\exp\left(-t/\tau_r\right)$ where τ_r is the recombination lifetime (Chithambo, 2007b). After the pulse, the luminescence is detected in addition to photomultiplier noise only and decreases in intensity with time which has the form of $I(t) \propto \exp\left(-\left(t-t_1\right)/\tau_r\right)$ where t_1 is duration of the stimulation pulse (Chithambo, 2007b). As it appears, stimulation and emission are separated in time in this method. An example curve obtained during stimulation and emission is shown in Fig. 3.13.

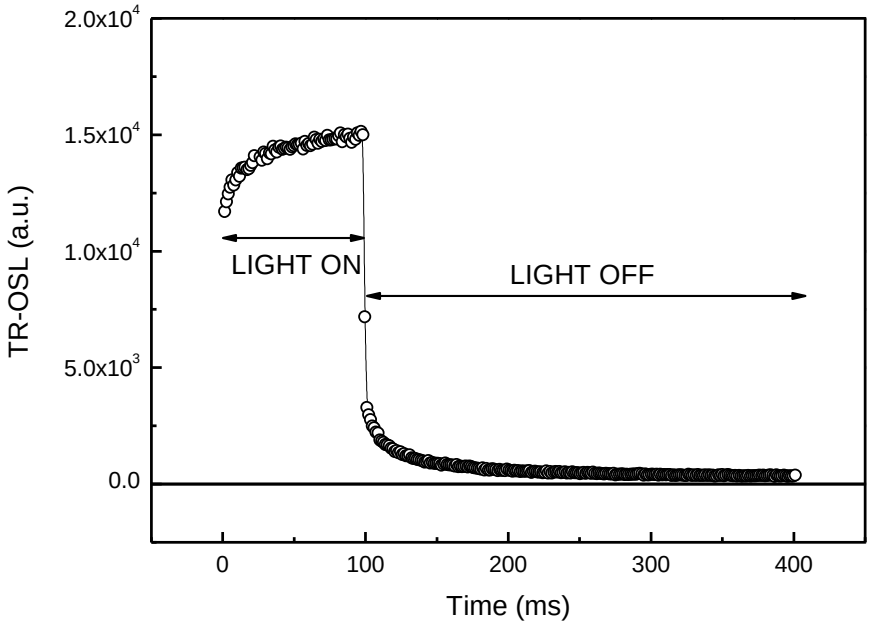

Figure 3.13 A typical TR-OSL signal.

There are three obvious advantages of TR-OSL. The first is that the signal-to-noise ratio remains high throughout the emission measurement. Because there is only photomultiplier noise accompanied with this measurement. The second one is that the electron population in the excited states of the luminescence center is essentially constant because of the short stimulating-light pulse. Thus, multiple signal measurements can be performed. The third and the most important one is that this technique enables us to study the luminescence lifetimes which is the delay between stimulation and emission of luminescence.

3.5 OSL and TL Dosimetry

OSL and TL have the same mechanism excluding the stimulation source as it has been mentioned before. Hence, they can be used for the same dosimetric purposes such as personal, environmental, medical and retrospective (dating, accident) dosimetry. Retrospective dosimetry can include evaluation of radiation absorbed by natural materials for purposes of luminescence dating. Similarly, environmental radiation dose occurred as a result of nuclear waste disposal, emissions from nuclear power, the nuclear weapons industry etc. is evaluated by using the natural minerals in environmental dosimetry. In another example of retrospective dosimetry, however, one is concerned with the doses absorbed by locally available materials during radiation accidents for the purposes of estimating the doses received by people during the exposure event. This could be described as an example of personal dosimetry. But, the OSL dosimeter used in personal dosimetry applications should be tissue equivalent. Medical dosimetry is also dealt with the dose of radiation exposed by a person. But, very small dosimeters capable of being used on or in (in vivo) the patient during medical radiation treatment and diagnosis are required in this application. For further detail about these dosimetric applications, the studies reported by Afouxenidis et al. (2007), Zacharias et al. (2007), Yukihara et al. (2010), Nascimento and Hornos (2010) can be referred.

CHAPTER 4

NATURAL FLUORITES

Fluorite which has a form of CaF_2 is a large-band gap insulator. It has a great many of properties indicated that it can be used in dosimetric applications. As well as this mineral is a well known TL dosimeter, its OSL properties reported recently (Chougaonkar and Bhatt, 2004; Polymeris et al., 2006; Yoshimura and Yukihara, 2006) have enhanced the probability of usability of this mineral as an OSL dosimeter. However, further OSL studies are required. Therefore, OSL properties of natural fluorites were investigated in detail in this study. But, before explaining the results obtained from these investigations, general properties of natural fluorites will be discussed throughout this chapter.

4.1 Crystal Structure and Defects

It is important to know what the properties of the color centers (*F*- and *M*- centers) in CaF_2. But, before this, some lattice properties of this mineral should be summed up in note. CaF_2 is a face-centered cubic, experimental lattice constant of which is 5.4630 Å (Wyckoff, 1963), large-band gap insulator. Its lattice structure is shown in Fig. 4.1. It has experimentally observed that its direct band gap is 12.1 eV (Rubloff, 1972).

The earliest work on color centers in CaF_2 was carried out by Mollwo (1934) and Przibram and collaborators (1956, 1959). Mollwo (1934) was studied the additively colored natural fluorite crystal and found two prominent absorption bands at 375 nm and 520 nm which he called them the α and β bands shown in Fig. 4.2. He has suggested that the α band was due to the *F*-center and Arends (1964) showed that the absorption of the *F*-center occured in the α band region by using the optical measurements and electron spin resonance techniques. The energy levels of this center have also been calculated theoretically by Bennett and Lidiard (1965) and Feltham and Andrews (1965) for various alkaline earth fluorides. As a result they found 3.19 and 3.8 eV, respectively and these results verify the Arends' result which is 3.3 eV.

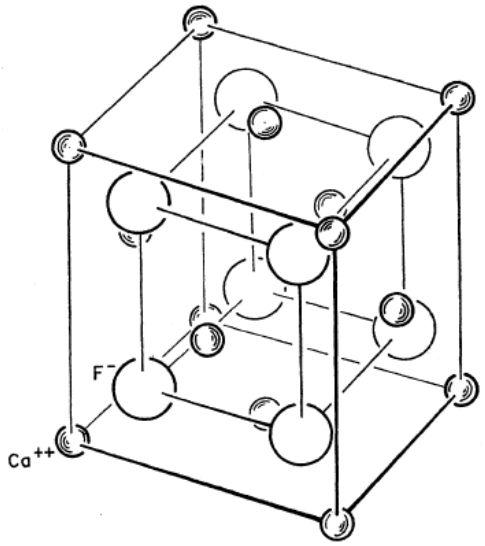

Figure 4.1 Fluorite structure (After, Scouler and Smakula, 1960).

It has been reported by various authors that the position of the peak of the α-band changes between 375 and 400 nm at 300 K. This seems depend on the coloration process, the treatment and the concentration of color centers. Przibram (1959) and Smakula (1954) indicated that this variation may be caused by small lattice distortion and the presence of impurities. For instance, when the fluorite crystal is colored in

Ca vapour, it shows an intense α-band at 375 nm, a β-band at 520 nm and three less intense bands at 600, 670 and 750 nm (Arends, 1964). Notwithstanding, CaF_2 crystal can be colored by X-rays and this coloration results in an α-band at 400 nm. Furthermore, it has been shown in the absorption spectra of the electrolytically colored CaF_2 that three absorption bands at 600, 670 and 750 nm are much more pronounced (Arends, 1964) as it is shown in Fig. 4.3. Arends (1964) supposed that this increase in intensity may be due to the action of H_2O and O_2. As shown by Bontinck (1958), a treatment of CaF_2 in air gives a partial decomposition to CaO, together with small amounts of $Ca(OH)_2$. A fraction of the produced O^{2-} ions replaces probably F^- ions. For each O^{2-} ion incorporated in the lattice an anion vacancy is formed. This process together with a distortion of the crystalline lattice will favor the production of complex centers.

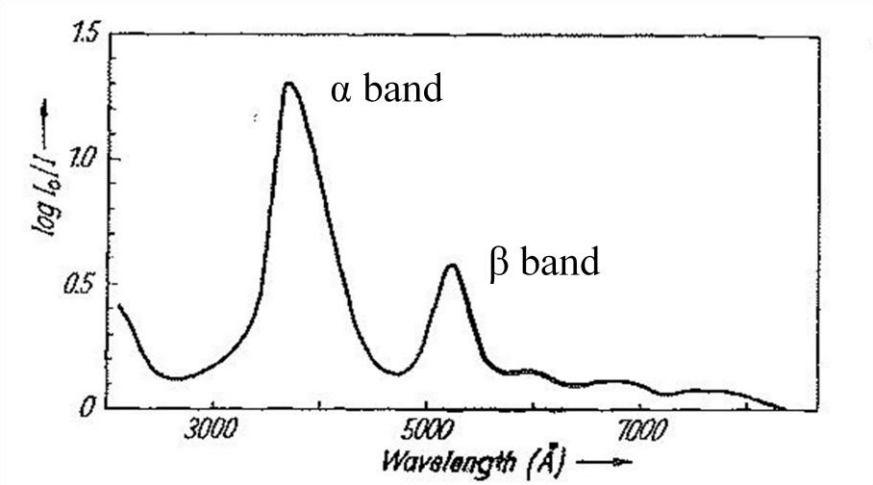

Figure 4.2 The optical absorption spectrum of an additively colored CaF_2 crystal at 300 °K (After, Arends, 1964).

After all of these studies, the α band has been shown to be a complex superposition of bands caused by the *F*-center, the *M*-center and higher *F* aggregate centers and the β band has been shown to be a band caused by the *M*-center by Beaumont and Hayes (1969). Therefore, these bands were re-called as S-band and M-band, respectively.

With the help of polarized bleaching and polarized fluorescence measurements, the *M*-center has determined as composed of two nearest neighbor *F*-centers and hence is aligned along <100>.

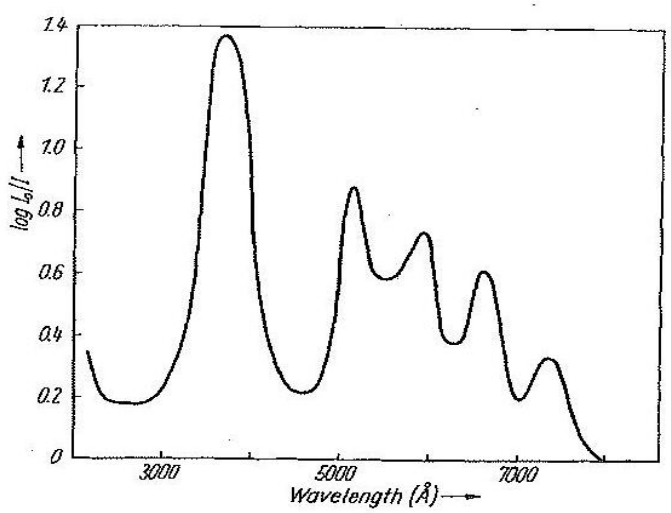

Figure 4.3 The optical absorption spectrum of an electrolytically colored CaF_2 crystal at 300 ^{o}K (After, Arends, 1964).

4.2 Optical Properties

Natural fluorite is probably the most colorful mineral. This can be because of impurity-associated defects or impurity ions as well as intrinsic defects such as *F*- and *M*- center. The structural defects have been explained up to now. Henceforth, the impurities caused for different colors in this mineral will be revealed with the optical absorption and emission spectrums reported.

Complex centers involving rare-earth ions and/or oxygen give rise to the various colors observed. These include yttrium-associated *F*-centers (blue), coexisting yttrium and cerium-associated *F*-centers (yellowish-green), the (YO_2) center (rose) and O^{3-} molecule ion (yellow). Divalent rare-earth ions also contribute to the

colorations, as for instance Sm^{3+} (green fluorites), or they are at the origin of strong fluorescence observed (Eu^{2+}). Furthermore, strong irradiation of the crystal with ionizing radiation leads to coagulation of color centers, and to precipitation of metallic calcium colloids.

There are two important properties of natural fluorite which give rise to the extraordinarily rich possibilities of creating color centers in this mineral. The first one is that the material easily incorporates cation impurities, especially rare-earth ions. The second, oxygen is introduced into the crystals without much difficulty at temperature down to 100 ºC by hydrolysis (Bontinck, 1958) and it is possible during hydrothermal growth processes. Direct reaction with oxygen also occurs, but this seems to proceed at a much slower rate than the hydrolysis reaction.

At this stage, it is important to know the role of the impurities on coloration. Calderon et al. (1992) have investigated the absorption, the emission and the excitation spectrum of natural fluorite crystals and correlated these spectra with results formerly reported for synthetic crystals. Optical absorption spectra which they obtained in the 200-800 nm wavelength range and at room temperature are shown in Fig. 4.4.

According to the spectrum obtained for the green fluorite (Fig. 4.4 (a)), there are a number of lines corresponded to different transitions between the $4f6$ and $4f5$ to the $5d1$ electronic configuration of Sm^{2+} (Kaiser et al., 1961; Loh, 1968, 1969; Vagin et al., 1969). Furthermore, the similarity of this absorption band to that reported for other natural green fluorites (Bill and Calas, 1978) have indicated that samarium is an important ion in the coloration in this kind of fluorite. As it shown in Fig. 4.4 (b), absorption spectrum of the yellow fluorite contains two bands at 300 and 434 nm. The latter has been related (Bill et al., 1967) with the presence of O^{3-} molecular ions substituting for two adjacent F^- ions (this has been named the YC

band or “Yellow Center”). The former band will be described during the discussion of the excitation spectrum. The Pink fluorite sample shows absorption bands at 220, 320, 410 and 530 nm (Fig. 4.4 (c)). Similar results have been reported by Hayes (1974) and Ehrlich et al. (1979) and related to the presence of (Y^{3+}-F) dipolar molecular centers. Lastly, the spectrum obtained for dark blue fluorite (Fig. 4.4 (d)) consists of narrow bands at 310 and 395 nm and a broad band between 560 and 580 nm. The broad band has been related to aggregated colloids of calcium atoms (Kubo, 1966; McLaughlam and Evans, 1968; Braithwaite et al., 1973). The colloid nature of the defect site was suggested by the fact that the width of the absorption band did not reduce during cooling from 300 to 77 K.

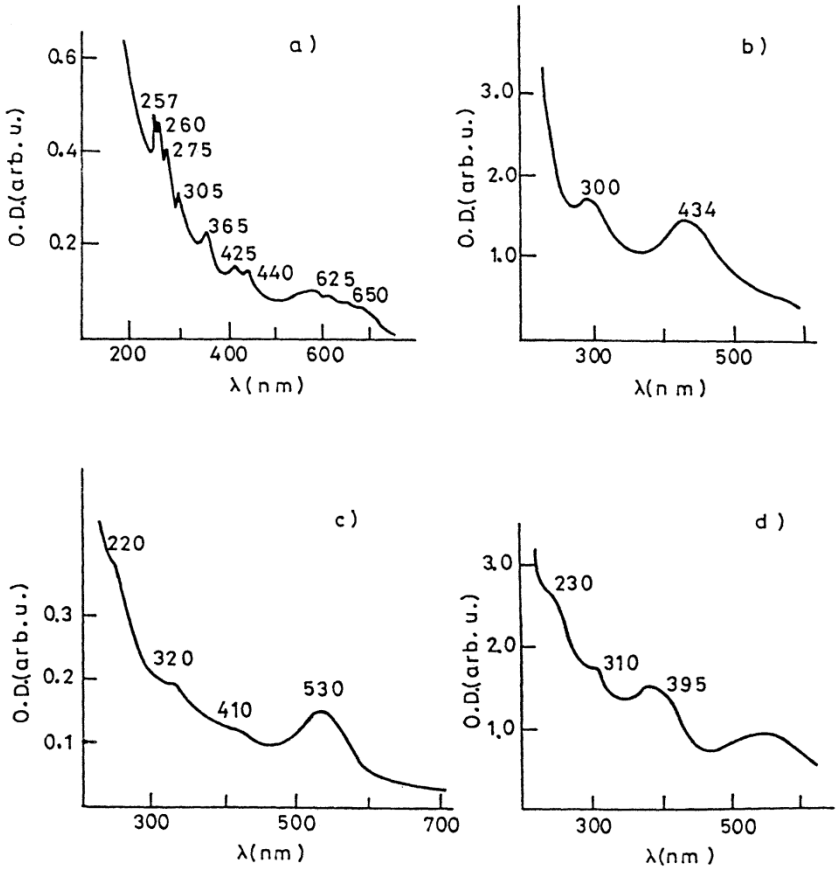

Figure 4.4 Absorption spectra at RT of natural fluorite crystals, Spanish (a) green fluorite from Badajoz; (b) yellow fluorite from Segovia and (c) pink material from Asturias. The dark blue fluorite (d) originated in the U.S.A. (After, Calderon et al., 1992).

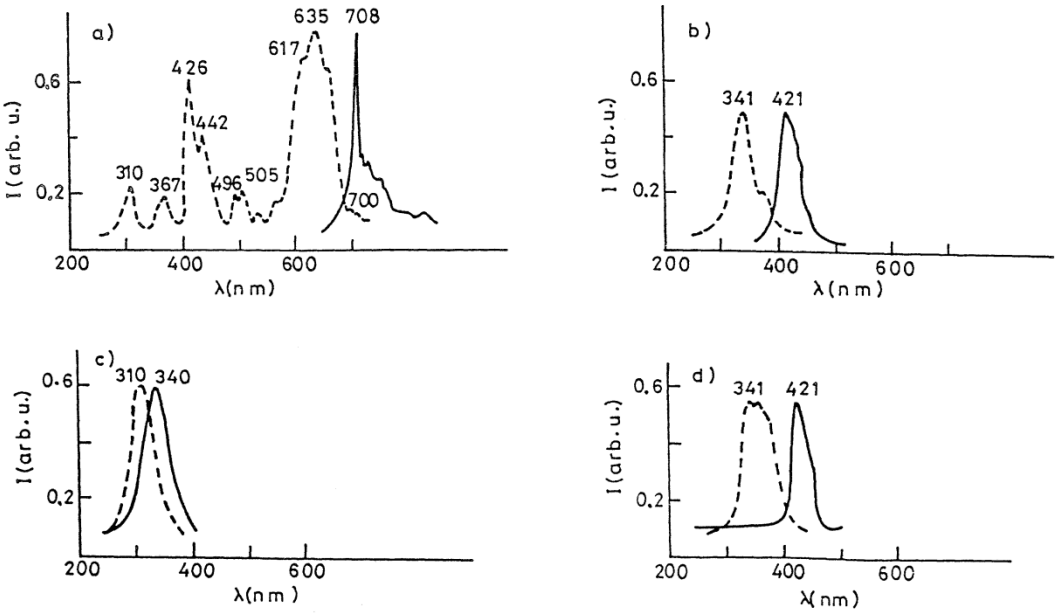

Figure 4.5 Photoluminescence spectra of fluorite. Dashed lines are the excitation spectra corresponding to emission at (a) 708.5 nm; (b) 421 nm; (c) 340 nm and (d) 421 nm. Full lines are the emission lines for excitation at (a) 426 nm; (b) 341 nm; (c) 310 nm and (d) 341 nm (After, Calderon et al., 1992).

Judging by the PL spectra (Fig. 4.5) obtained under excitation in the optical absorption region corresponding to Fig. 3.6 at 77 K, green sample shows a spectrum (Fig. 4.5 (a)) which is quite similar to that previously reported for CaF_2:Sm^{2+} synthetic crystals which show a maximum at 708.5 nm superimposed on a broad and structured emission band. This spectrum corresponds to the decay of the $5d$ and $4f$ transition of Sm^{2+}. In addition to that, excitation on the high energy side of the absorption band (< 341 nm) produces an emission band peaking at 421 nm (Fig. 4.5 (b)), which has been related with the signals for Eu^{2+} seen in doped synthetic crystals of CaF_2:Eu^{2+} (Loh, 1969). Emission spectra obtained for yellow sample which are illustrated in Fig. 4.5 (c) and (d) show emissions at 340 and 421 nm after excitation with light of wavelengths of 310 and 341 nm, respectively. These have been identified with the transitions from $5d$ to $4f$ and from $4f6$ or $5d1$ to $4f7$ of Ce^{3+} (Ehrlich et al., 1979) and Eu^{2+} (Murrieta et al., 1983), respectively. No emission was

detected for pink and dark blue fluorites under excitation with the wavelengths they studied.

Finally, the excitation spectra corresponding to the above emission bands have been reported. These spectra are shown in Fig. 4.5. The peaks corresponding to the e_{2g} symmetry component shown in the excitation spectrum for the green fluorite of the 708.5 nm emission band (Fig. 4.5 (a)) have been labeled in terms of the electronic levels of the $4f5$ configuration following the work of Loh (1968) in synthetic $CaF_2:Sm^{2+}$ crystals. Fig. 4.5 (b) also includes the excitation spectrum of the green fluorite corresponding to the Eu^{2+} emission. A broad and structured band at 340 nm have been corresponded to one of the two absorption bands reported for synthetic Eu doped CaF_2 crystals (Kobayasi et al., 1980). Yellow sample shows two kinds of excitation spectra which have been corresponded to 340 and 421 nm emission wavelengths (Fig. 4.5 (c)). The first one is composed of one band at 310 nm that has been related with $5d$ to $4f$ ion transitions of Ce^{3+} (Ehrlich et al., 1979) and a secand is centered at 341 nm and arises from the $4f6$ or $5d1$ to $4f7$ levels of Eu^{2+} (Murrieta et al., 1983).

As a result of these studies, it has been shown that green samples contain Sm^{2+} and Eu^{2+}; yellow samples contain Ce^{3+} and the "YC" defects; pink ones include (Y^{3+}-F) and dark blue samples have Ca aggregated colloids.

4.3 Dosimetric Properties

Natural CaF_2 is a well-known thermoluminescent material. The TL properties of this mineral in both natural and synthetic form have been extensively reported (Balogun et al. 1999; Nambi 1975; Sunta 1984; Urbina et al., 1998; Sohrabi et al., 1999; Topaksu and Yazıcı, 2007) as it has been previously mentioned. However, there are

few studies reported about the OSL properties of natural fluorites (Chougaonkar and Bhatt, 2004; Polymeris et al., 2006; Yoshimura and Yukihara, 2006).

Chougaonkar and Bhatt (2004) have investigated the OSL properties of natural fluorites and they have tried to find relation between the OSL decay curve and the TL peaks of this mineral. They have concluded that the OSL signal of this sample is caused by the traps responsible for the first three TL peaks which are occurring at 126 ˚C, 196 ˚C and 264 ˚C with 5 °Cs^{-1} heating rate. Likewise, Linear-Modulation-OSL (LM-OSL) signal has been investigated and it has been found that the traps responsible for the first TL peak are the same as those causing the first LM-OSL peak. Again, the second LM-OSL peak has been found to be caused by the traps which are in charge of the second and third TL peaks.

Later, Polymeris et al. (2006) have investigated the OSL sensitivity and the lowest detectable dose limit (LDDL) of natural fluorite and they have compared the OSL properties with that of TL. It has concluded from the growth curve that the LDDL is roughly of the order 10^{-6} Gy for OSL as the same as the LDDL found for TL before this study (McKeever et al., 1995; McKeever, 1985; Becker, 1973). They have also observed that the OSL signal of natural fluorite has four components which are termed as ultra-fast, fast, medium and slow. The sensitivity changes of the TL peaks and these OSL components as a function of successive TL and OSL readout cycles has been monitored. The ultra-fast and the fast component have been shown to be stable, whereas the medium component has been shown to be relatively stable. The slow component, however, has been shown to be highly sensitized. This has been attributed to its incomplete bleaching after each cycle. In the case of TL, sensitivity of all of the TL peaks which are around 90 ºC, 183 ºC, 275 ºC (with 1 °Cs^{-1} heating rate) was found to be stable. The absence of thermal quenching in this phosphor has been revealed by observing the stability of integrals of all glow peaks as a function of the heating rates. It has also been shown that CW-OSL signal increases as a function of temperature exponentially which corresponds to thermally activated processes with the activation energy is 0.368 ± 0.006 eV. Similarly, a thermally activated

photo-transferred TL effect has been observed by investigating the residual TL signal as a function of illumination time obtained after CW-OSL measurements.

Among the recently reported studies, natural fluorites have also been investigated by Yoshimura and Yukihara (2006). They showed that the OSL signal obtained by stimulation with blue light is very intense. Furthermore, it has been observed that if pre-annealing is done at 150 ˚C, the intensity of this signal does not change with time delays at least 2000 s.

These reported OSL properties are not sufficient to decide whether this mineral is suitable for use as an OSL dosimeter in environmental dosimetry applications or not. Therefore, the dosimetric properties of natural fluorites using OSL have been investigated in details and the results of these investigations will be discussed in Chapter 6.

CHAPTER 5

EXPERIMENTAL PROCEDURES AND TECHNIQUES

As stated before, the purpose of this thesis is to investigate OSL properties of natural fluorites which have different colors. For this purpose, X-ray diffraction patterns, OSL signals, TL signals and TR-OSL signals of these samples were obtained and analyzed. The equipments and the techniques used will be explained throughout this chapter.

5.1 Sample Preparation

Four natural fluorite samples (Fig. 5.1) of different origins were used in this study. These origins and the colors which they include are presented in Table 5.1. These fluorite samples were renamed as V-Fluorite (violet part of the sample shown in Fig. 5.1 (a)), T-Fluorite (transparent part of the sample shown in Fig. 5.1 (a)), K-Fluorite (Fig. 5.1 (b)), Y-Fluorite (Fig. 5.1 (c)) and G-Fluorite (Fig. 5.1 (d)) for simplification.

To prepare these samples for measurements, firstly, all of the fluorite samples were cleaned with alcohol except that the K-fluorite was treated by hydrochloric acid (HCl) because it also had calcium carbonate mineral ($CaCO_3$) and then it was cleaned by means of ultrasonic cleaner. Later, these samples were crashed and

powdered. The samples in powder form were fixed on 10 mm diameter aluminum discs by silicon oil.

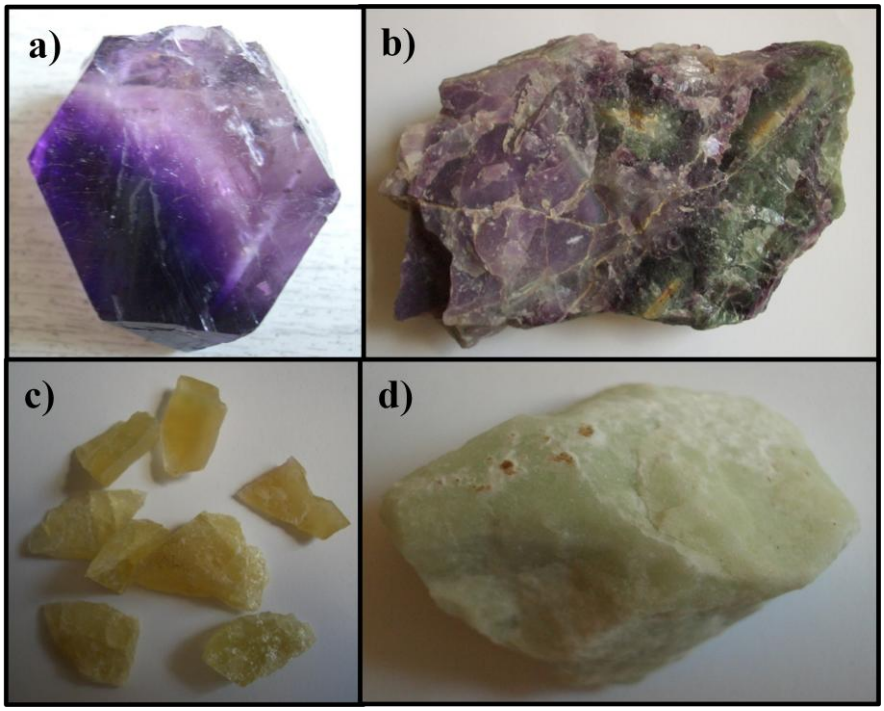

Figure 5.1 Natural fluorite samples used in this study: a) V-Fluorite and T-Fluorite; b) K-Fluorite; c) Y-Fluorite; d) G-Fluorite.

Table 5.1 Origins and colors of natural fluorite samples.

Natural Fluorite Sample	Location	Color(s)
V-Fluorite	U.S.A.	Violet, Transparent
K-Fluorite	Turkey	Violet, Green
Y-Fluorite	China	Yellow
G-Fluorite	Turkey	Green

5.2 X-Ray Diffraction Experiments

X-ray diffraction (XRD) patterns were obtained to verify that the samples are calcium fluoride (CaF_2). One of them which was obtained for K-fluorite is shown in Fig. 5.2. This experiment was performed using a "Rigaku Miniflex" diffractometer with CuK_α radiation having a wavelength of 1.541838 Å. Diffraction angle (2theta) range was taken between 5-70˚ at scan speed of 1˚ min^{-1}. According to the findings, all samples used in this study which were renamed as V-fluorite, T-fluorite, K-fluorite, Y-fluorite and G-fluorite are calcium fluorides the lattice constant of which equals to 5.462 Å and it was also found that their bravais lattices are face-centered cubic.

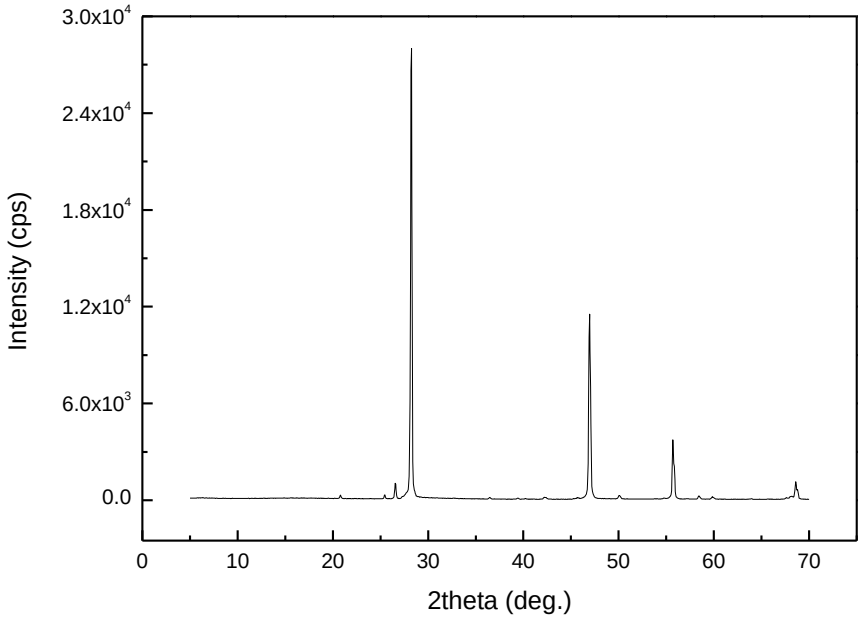

Figure 5.2 XRD pattern of the K-fluorite at room temperature.

5.3 CW-OSL Experiments

In the equipment used for CW-OSL experiments, the irradiated sample is stimulated continuously with light and emitted photons (OSL) is detected by a photomultiplier tube (PMT) as pulses which is then monitored on a PC. This process has been explained schematically in Fig. 5.3.

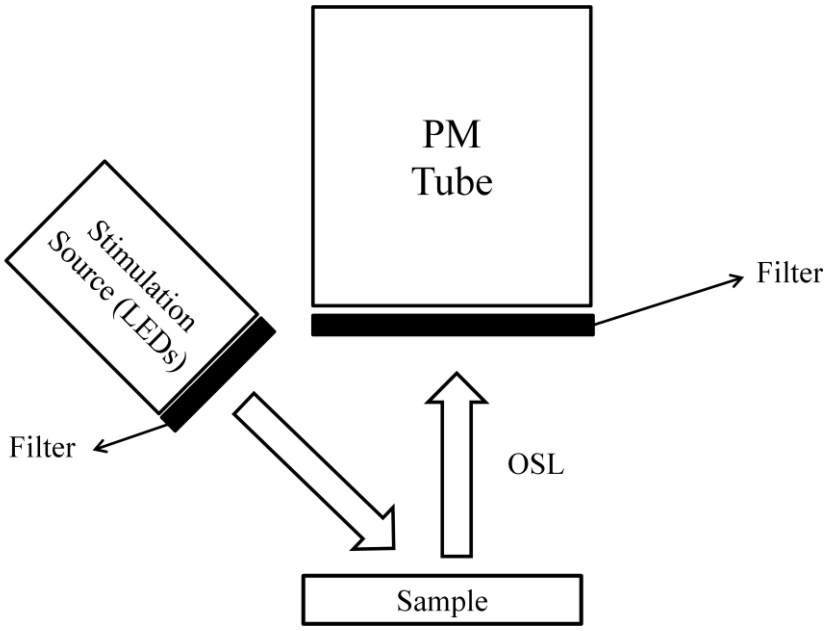

Figure 5.3 Schematic representation of a CW-OSL measurement system.

OSL signals were obtained by an ELSEC model 9010 type OSL measurement system. It is an apparatus developed in collaboration of Littlemore Scientific Engineering (ELSEC). However, there has been a change in stimulation unit of the system. A WENRUN type LUB20043 blue LEDs mentioned in the study by Eygi et al. (2007) have been used throughout this study. Peak wavelength of these LEDs is ~ 470 nm and power density is 35-40 mW/cm^2 at the sample position. The filter in front of the LEDs is Schott GG-420 which has a transmission wavelength longer than 420 nm.

Electron Tubes Inc. 9235 QB PMT, which is the component of the equipment having a bialkali photocathode, was used in the detection part. The filters in front of these PM tube are two U-340 Hoya filters. This filter has a transmission mainly between 280 nm and 380 nm.

Irradiations were performed by Sr^{90}/Y^{90} beta source (dose rate ~ 0.033 Gy/s) which is the removable part of the CW-OSL equipment. Also, NUVE EV 018 oven was used for preheating and heating at higher than preheat temperature was performed using CSF 1100 model Carbolite furnace.

5.4 TL Experiments

The TL signals were obtained by TL/OSL-DA-20 Model Risø TL/OSL Reader that is located in Institute of Nuclear Science at Ankara University. Either TL or OSL measurements can be performed using this equipment. Sr^{90}/Y^{90} beta source (dose rate ~ 0.15 Gy/s) is used for irradiation and the detection is performed by Electron Tubes Inc. 9235 QB PMT having a bialkali photocathode sensitive in 200-400 nm. In stimulation part, there are adjustable two sources of stimulation which are infrared and blue light. For further detail about this equipment, one can refer to the thesis reported by Kaya (2009).

The stimulation for OSL signal measurements was performed with blue LEDs which have a 470 nm wavelength and Hoya-U340 filter was used for detection the emission of TL and OSL in this study. Also, unless otherwise stated, all TL measurements were performed at a heating rate of 1 ˚C/s.

5.5 TR-OSL Experiments

TR-OSL system developed in Thermally and Optically Stimulated Luminescence Laboratory (TOSL) at METU was used to obtain TR-OSL signals. OSL stimulation was made by a blue laser diode module with 445 nm wavelength and ~ 14 mW/cm^2 optical power density (Power Technology Inc. IQ1C16). In front of this stimulation source, there is Schott GG420 filter to filter out short wavelength radiation from laser. A Hamamatsu R928 PMT having a multialkali photocathode sensitive in 185-900 nm is used for detection the luminescence through Schott DUG11 + Hoya U340 filters with a transmission range of 280-380 nm. PMT converts the individual luminescence photons into analog pulses. Then, these pulses are counted by SR-430 Multichannel scaler (Stanford Research Systems), and these counts monitored on PC on a time scale. There is also control electronics (Driver-DAQ Card NI6602) in the OSL stimulation unit which controls the laser driver for opening and closing of the laser. Schematic representation of the TR-OSL system is shown in Fig. 5.4.

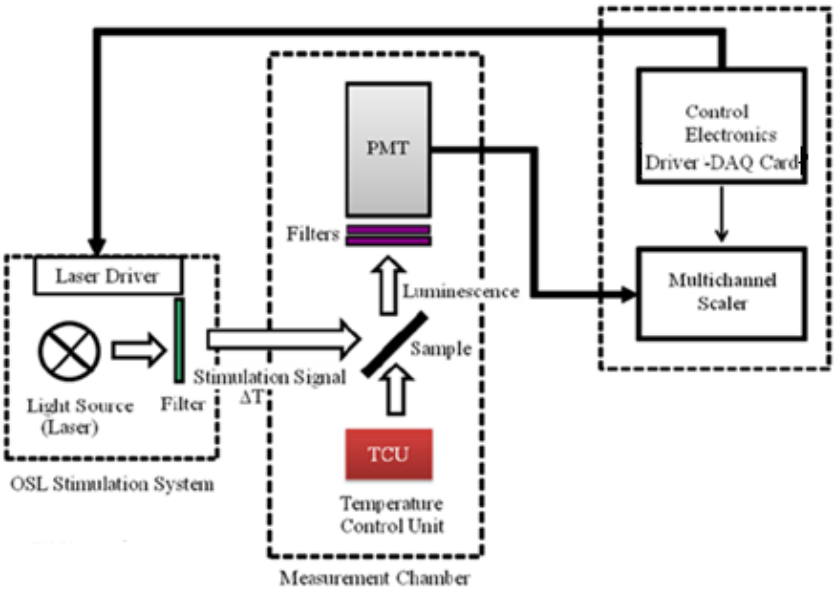

Figure 5.4 Schematic representation of TR-OSL system in TOSL at METU (Re-drawn after, Yeltik, 2009).

CHAPTER 6

RESULTS AND DISCUSSIONS

With the aim of checking the possibility of using OSL signal of natural fluorites for dosimetric purposes, characteristics of the OSL signal were investigated. In the following paragraphs, experiments carried out to reach this aim and their results are discussed.

6.1 Determination of an Appropriate Annealing Procedure

Before a detailed investigation on the OSL properties of natural fluorites, OSL signals induced during geological times should be deleted. For this purpose, using the temperature quoted in the literature (Sohrabi et al., 1999; Topaksu and Yazıcı, 2007), 500 ˚C, the annealing times were studied for the samples. The samples excluding the K-fluorite were annealed at this temperature for different time intervals and OSL was measured for 150 seconds at room temperature for various annealing time. The results are shown in Fig. 6.1. These plots were obtained after integrating the first 10 seconds of the OSL signal obtained for each annealing time. Also, same measurement was performed for 5 aliquots to observe the scattering from the mean value.

As seen in figure, for the V-fluorite and T- fluorite, an appropriate annealing time is ~ 45 hour, and for the G-fluorite and Y-fluorite, it is ~120 hour. It should be noted that the K-fluorite was not used in this experiment because it includes violet and green colors which were already investigated for this purpose. In a separate annealing experiment, it was found that ~ 45 hour annealing time is enough for this sample to remove the geological signal. The samples which were annealed in this way in a furnace were used in the following experiments.

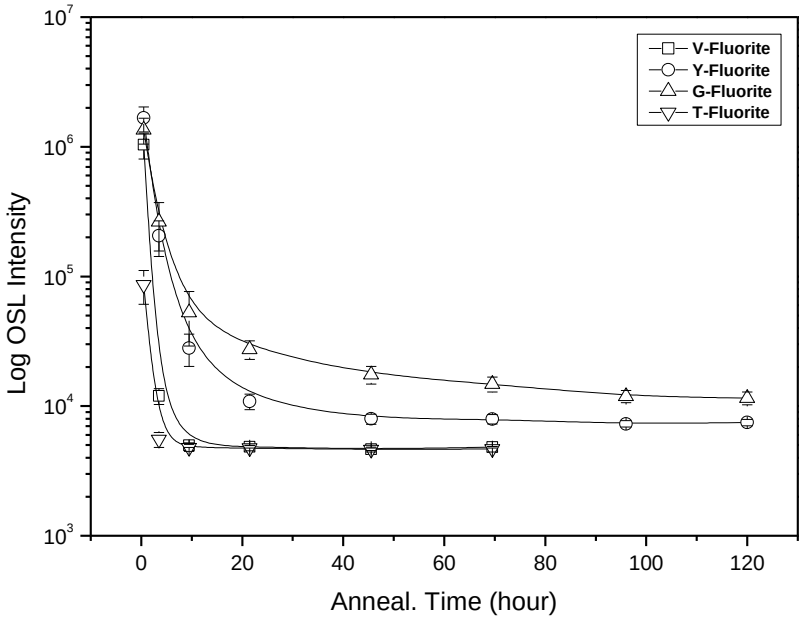

Figure 6.1 OSL responses of natural fluorites as a function of annealing time. Error bars represent 1σ standard deviation of 5 measurements.

6.2 TL Signals

In order to obtain an information about the traps and their distribution, TL glow curves of five samples were measured. TL measurements of 150 mGy irradiated aliquots made by linearly heating the aliquots to 450 ˚C. Representative TL glow

curves are shown in Fig. 6.2. As seen from the figure, for all five samples, these curves contain three main peaks located around 100, 190 and 300 ˚C, respectively. Peaks around 300 ˚C are composed of overlapping peaks which are marked with arrows in Fig. 6.2. Measured peak temperatures are summarized in Table 6.1. These results virtually act in accordance with those obtained by Polymeris et al. (2006), and Topaksu and Yazıcı (2007) for the fluorite samples of different origin.

Comparing the peak temperatures of TL curves of fluorites, it is probable that they are related to similar types of electron traps. Besides, low temperature peak related to shallow traps ends at ~ 160 ˚C for the K-fluorite and at ~ 140 ˚C for the rest samples. This means that the samples should be heated up to these temperatures to remove the contribution of shallow traps. This was performed in experiments discussed in section 6.5 and 6.12. Also, as it appears from the Fig. 6.2, the traps related to three main peaks are depleted when the samples are heated up to 450 ˚C. In experiments described in section 6.3, 6.5, 6.10 and 6.12, this heating scheme was used before each OSL measurement because the samples were heated at linear heating rate. However, the samples were heated at 400 ˚C for 30 minutes in a furnace for remaining experiments.

Table 6.1 TL peak temperatures of natural fluorites. The third peaks are composed of overlapping peaks.

Natural Fluorite Samples	1. Peak	2. Peak	3. Peak
Y-Fluorite	95 ˚C	190 ˚C	285˚C
G-Fluorite	97 ˚C	198 ˚C	319 ˚C
K-Fluorite	115 ˚C	200 ˚C	300 ˚C
V-Fluorite	92 ˚C	193 ˚C	300 ˚C
T-Fluorite	88 ˚C	187 ˚C	295 ˚C

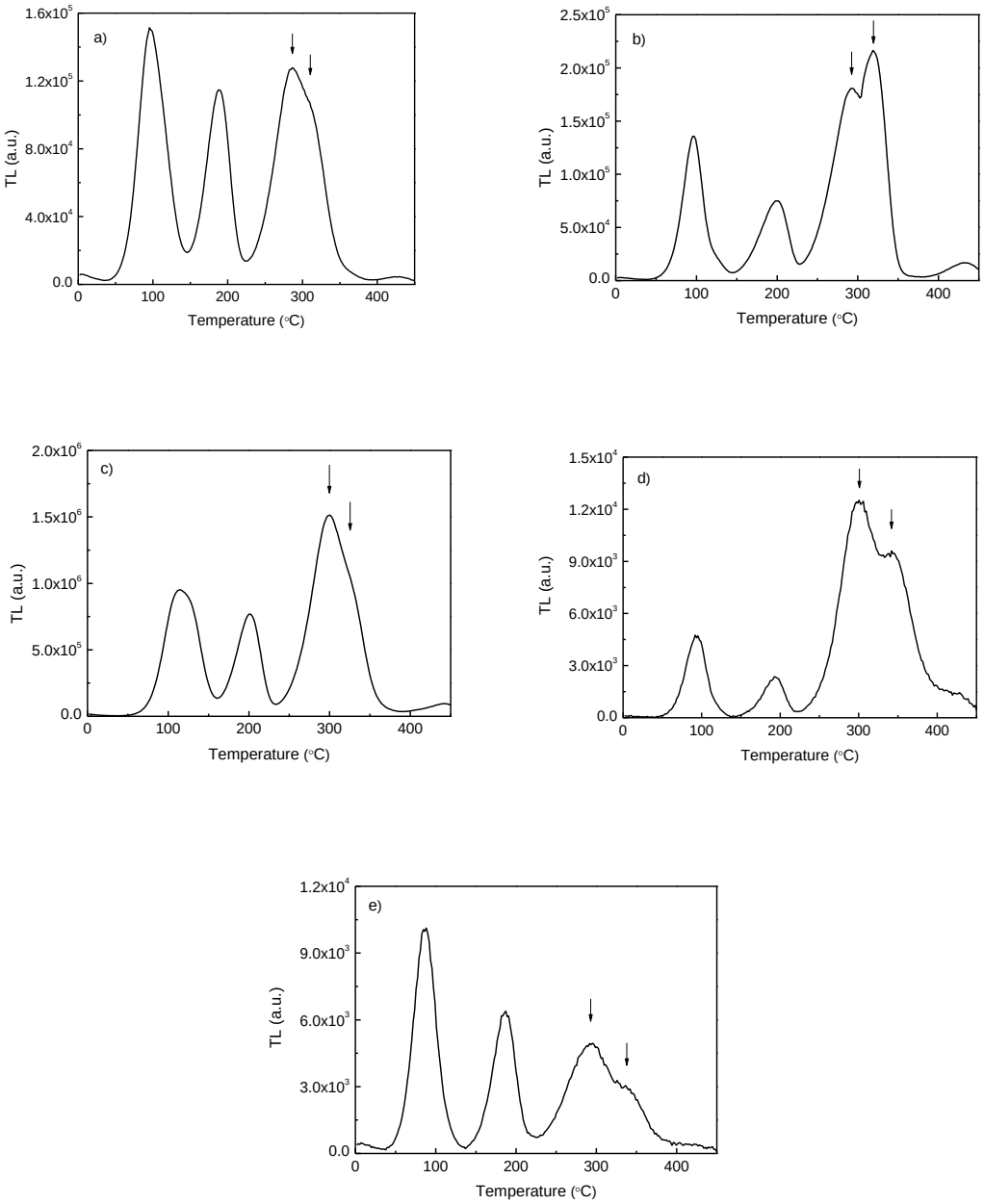

Figure 6.2 TL Glow curves of natural fluorites for 150 mGy β doses: a) Y-Fluorite; b) G-Fluorite; c) K-Fluorite; d) V-Fluorite; e) T-Fluorite.

6.3 Determination of an Appropriate Preheat Temperature

Preheat helps to remove the contribution of the unstable traps, generally appearing at low temperatures in a TL glow curve, from the OSL signal. An appropriate preheat temperature was searched by heating the samples to various temperatures at a heating rate of 1 ˚C/s in the range 50-350 ˚C with 10 ˚C steps after irradiation with 150 mGy beta doses. After each preheating, OSL was monitored with brief (0.1 second) pulses at room temperature. Each OSL measurement was followed by a preheat procedure at a successive temperature. Because the irradiation was performed once throughout the experiment, correction was made for the loss of OSL signal during the short pulses considering the loss of the OSL intensity in decay curve. Plots obtained as a result of this process are shown in Fig. 6.3. The OSL responses for low temperatures near to room temperature are not included in the graphs as they have very high intensities because of high electron population in the shallow traps.

According to the plots given in Fig. 6.3, ~ 160 ˚C is an appropriate preheating temperature for the K-fluorite and ~ 150 ˚C for the others by considering the "plateau regions" of the graphs. These results act in accordance with those found from the TL glow curves in section 6.2. In a study on Brazilian calcium fluoride, Yoshimura and Yukihara (2006) have also shown that if the samples are heated to 150 ˚C after irradiation, there is no change of intensity with time delays of at least 2000 seconds. Hereby, preheating procedure was decided to be performed at 150 ˚C for 15 minute in an oven for the following experiments excluding the one discussed in section 6.5.

It was also observed from the graphs that there may be thermal transfer effects on the OSL signals, especially on those of V-and T-fluorites, since an increase was observed in low temperature part of their OSL versus preheat temperature plots.

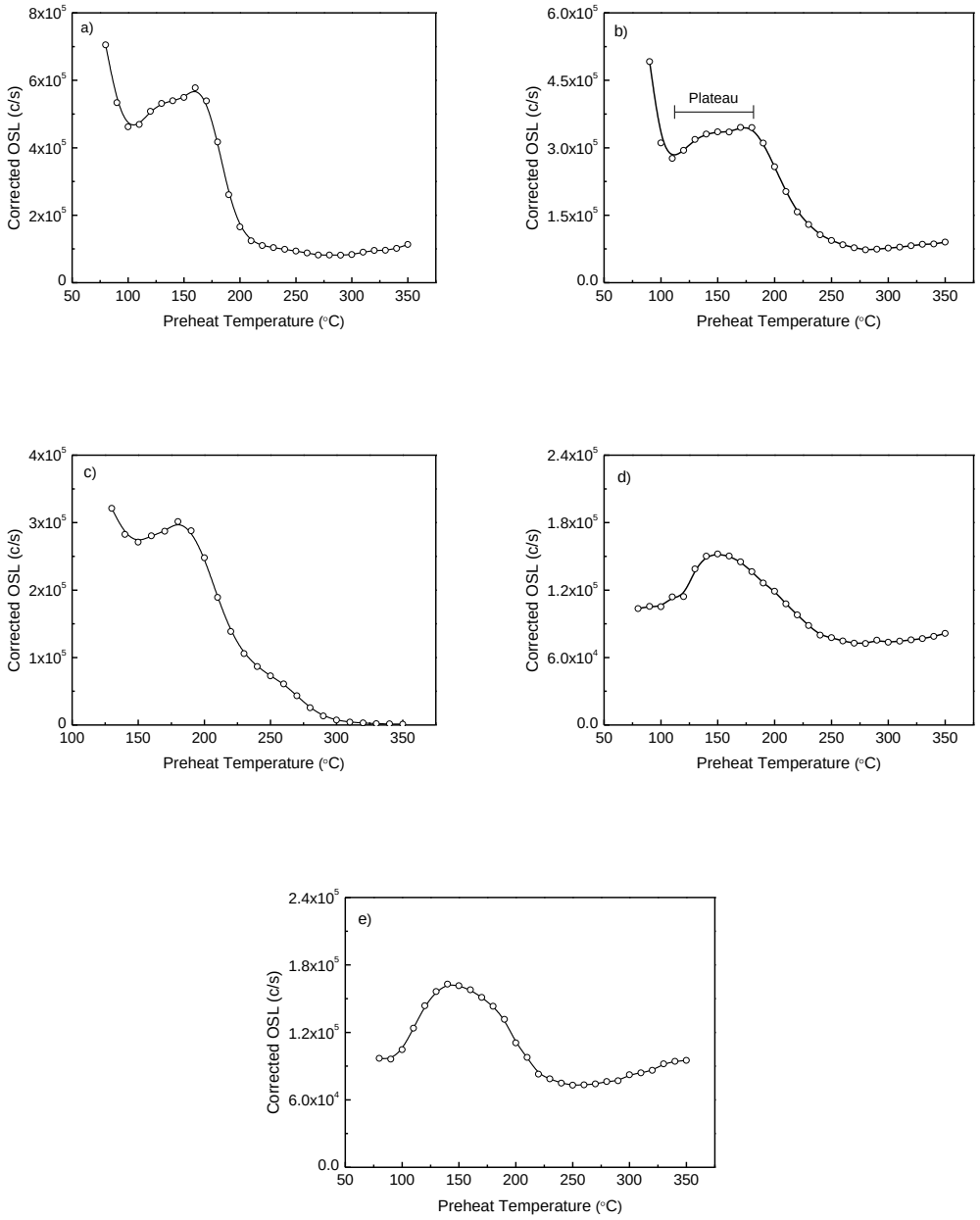

Figure 6.3 OSL responses of natural fluorites as a function of preheat temperature: a) Y-Fluorite, b) G-Fluorite, c) K-Fluorite, d) V-Fluorite, e) T-Fluorite.

6.4 OSL Signals

After obtaining appropriate parameters (annealing, preheat, post-annealing temperatures and annealing time), OSL signals for 100 mGy irradiated natural fluorite samples were measured for 750 seconds at room temperature (Fig. 6.4). As shown in the figure, all of the signals exhibit a monotonic decay. Furthermore, these signals were best fitted to the equation which is $I = I_0 + I_{01} \exp\left(-t/\tau_1\right) + I_{02} \exp\left(-t/\tau_2\right)$, where I_0, $I_{01,2}$ and $\tau_{1,2}$ are the background value, the initial intensity of the components of the signal and the decay constants, respectively (Fig. 6.4). From these fitting results, it may be said that the OSL signals are composed of a slow and a fast components.

If the decay constants (τ_1 and τ_2) given in labels of Fig. 6.4 are compared, it can be said that the OSL traps of the samples of different colors are comparable. The decay constant of slow component changes between 140-180 seconds and that of fast component changes between 18-28 seconds. Thus, OSL signals may be caused by the similar electron traps as is the case in TL signals discussed in Section 6.2.

It should be noted that unless otherwise stated, in the following experiments OSL signal intensities are obtained by subtracting the sum of the last 5 seconds from the sum of the first 5 seconds of the OSL signal.

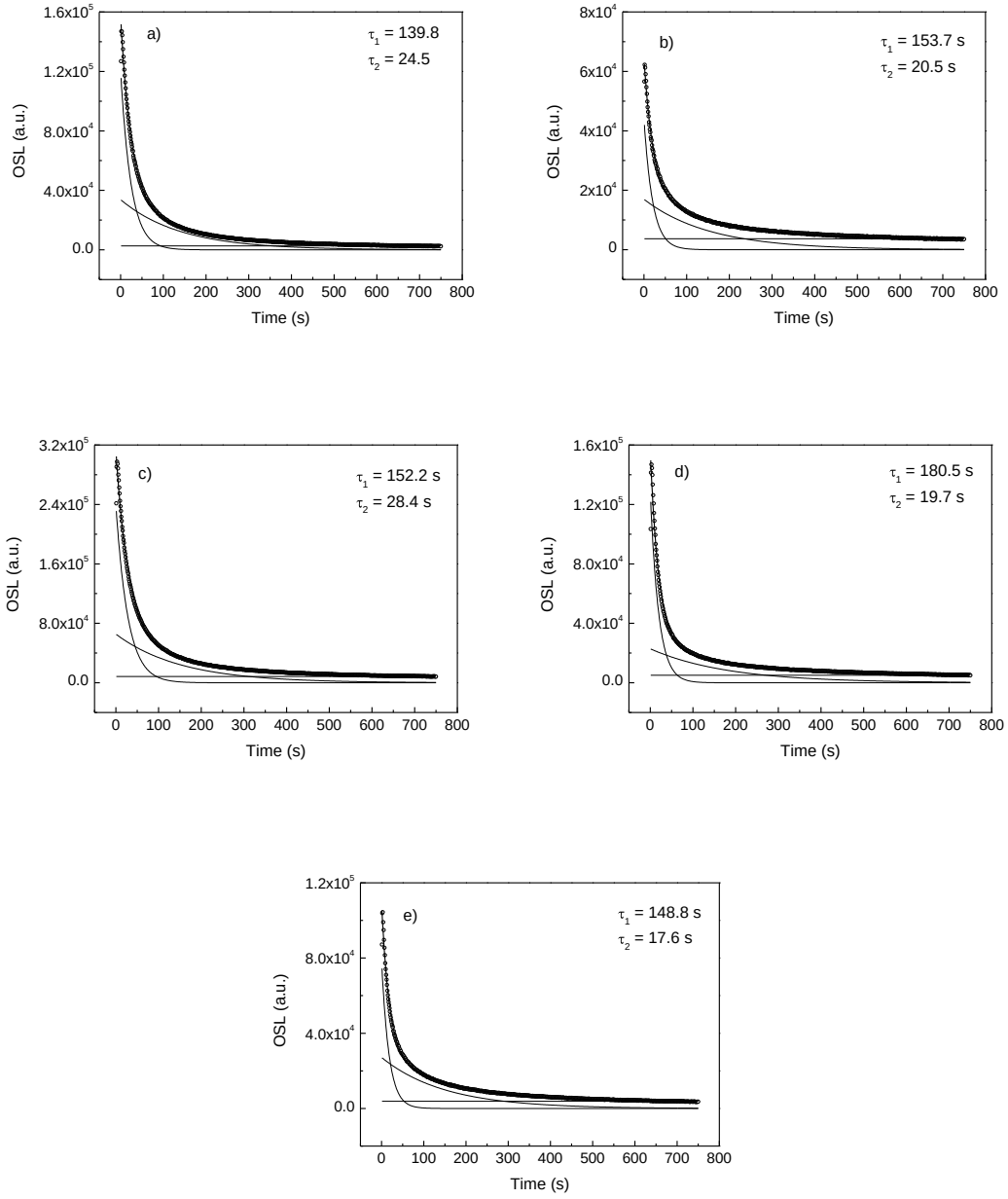

Figure 6.4 OSL signals and their components of natural fluorites for 100 mGy β doses: a) Y-Fluorite; b) G-Fluorite; c) K-Fluorite; d) V-Fluorite; e) T-Fluorite. Labels are the decay constants obtained by curve fitting.

6.5 Effect of OSL Measurement on TL Signals

This experiment was performed to investigate the optically active peaks of the TL glow curves. Thence, the TL signal obtained after OSL signal measurement for 300 seconds was compared with the TL signal obtained without measuring the OSL signal. Then, the first measurement was subtracted from the second one to obtain the signal only caused by optically active traps. The graphs obtained are presented in Fig. 6.5. It should be noted that OSL signal was depleted in 300 seconds in the equipment used in this experiment because of the high optical power density of the stimulation source of the Risø reader.

According to graphs, all of the TL peaks are affected from the optical stimulation. Hence, it can be said that these peaks involve optically active parts. Nonetheless, as seen, all TL peaks are bleached excluding the high temperature peaks of the V-fluorite (Fig. 6.5 (d)) and the T-fluorite (Fig. 6.5 (e)). These peaks are increased after the OSL readout. This may be because of re-trapping of the charges at deeper traps during the optical stimulation.

Thermal activation energies of the bleached peaks appearing around 190 °C which are calculated using the initial rise method will be discussed in Section 6.9. Then, these results will be compared with the energies obtained for the OSL traps to discuss the contribution of the OSL traps to the TL signals.

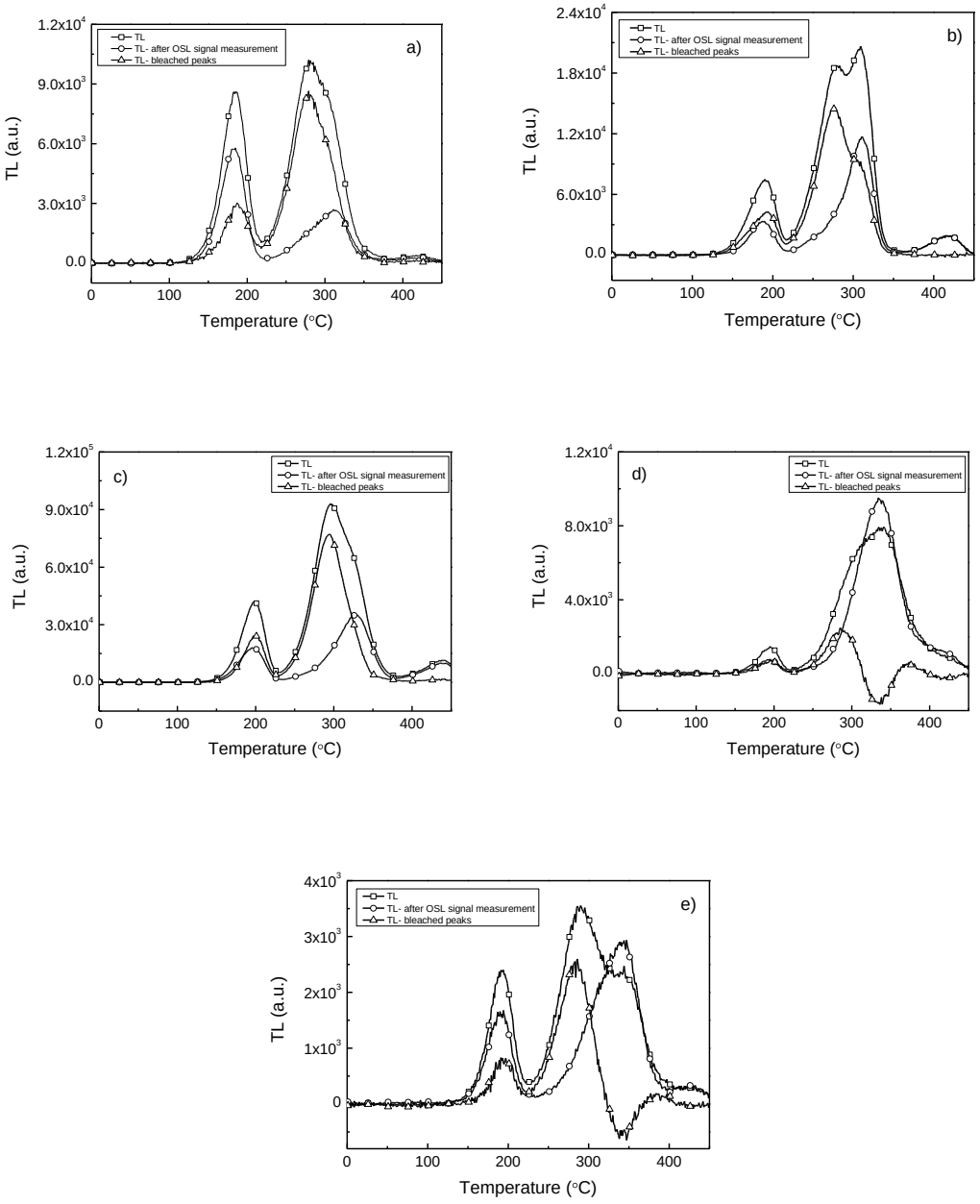

Figure 6.5 The effect of OSL measurement on TL signals of the natural fluorite samples: a) Y-Fluorite; b) G-Fluorite; c) K-Fluorite; d) V-Fluorite; e) T-Fluorite. The graphs labelled as a, b, c were obtained for 150 mGy β doses and the graphs labelled as d, e were obtained for 750 mGy β doses to observe the bleached peaks better.

6.6 Dose-Response of the OSL Signals

Dose-response of the OSL signals of the fluorite samples were checked in the range between 100 mGy and 100 Gy beta doses. OSL signals were measured for 750 seconds at room temperature for each dose. Plots of OSL intensities as functions of radiation dose together with the model equations and parameters obtained by curve fitting are given in Fig. 6.6. As seen from the figure, Y-and K-fluorites show linear response to radiation dose. However, V-and T-fluorites show a non-linear behavior. Dose response of both samples could be approximated using a saturating exponential function of the form $I = I_0\ 1 - e^{-D/D_0}$, where D_0 is the saturation dose and I_0 is the maximum OSL intensity. Saturation doses were obtained as ~ 24 and ~ 43 Gy for the V-and T-fluorites, respectively. Furthermore, dose-response of the G-fluorite was found to be slightly non-linear with a power factor of 1.1 instead of 1.0.

Polymeris et al. (2006) investigated the OSL dose-response curve of a natural fluorite by exposing the sample to the background environmental radiation for time intervals ranging from 1 to 15 days, where the environmental radiation level was found to be 225 nGy/h and they have shown that the growth curve becomes linear for doses larger than 10^{-5} Gy. If it is assumed that the samples investigated in this study have the same response, it can be concluded that natural fluorite samples have a linear response in a wide range. Furthermore, lowest detectable dose limit (LDDL) was calculated for each sample assuming that the intensity corresponding to this dose is two times of the zero dose OSL reading. As a result, it is found to be roughly of the order 10^{-2} Gy for each sample. However, it is found to be of the order 10^{-6} Gy in the study reported by Polymeris et al. (2006) for different fluorite samples. To obtain more reliable results for LDDL, the response of the samples to the background environmental radiation for different time intervals will be studied in detail.

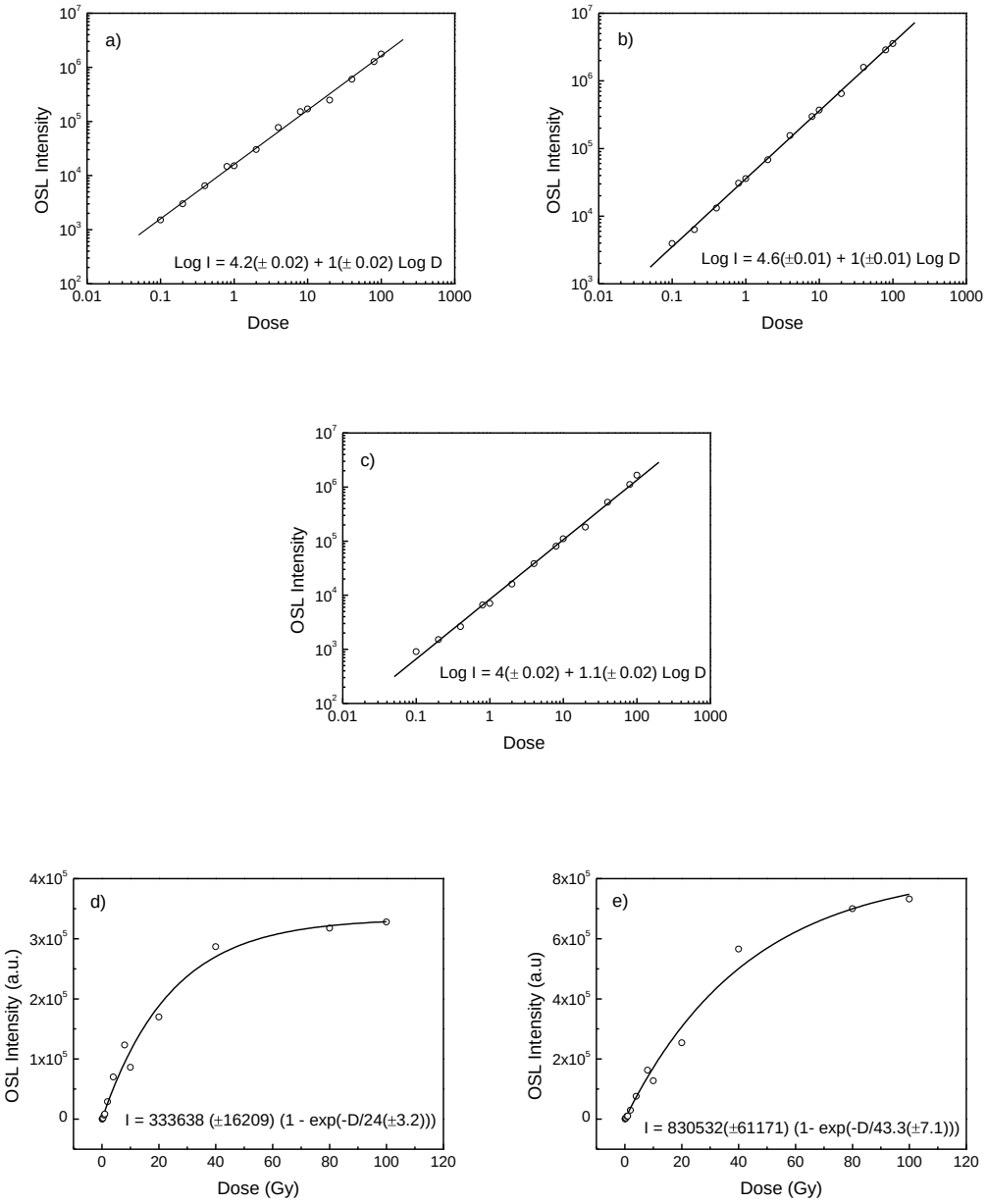

Figure 6.6 Dose-response of the OSL signals of the natural fluorite samples: a) Y-Fluorite; b) K-Fluorite; c) G-Fluorite; d) V-Fluorite; e) T-Fluorite.

6.7 Reproducibility of the OSL Signals

For a dosimetric application, the OSL measurements must be reproducible. In other words, the signal must show the same response, when it is re-measured under the same conditions. To test the reproducibility, the signal was measured for 750 seconds at room temperature for 100 mGy beta doses and this measurement scheme repeated 5 times. Then, the OSL intensity was plotted versus number of measurements (Fig. 6.7). As shown in figure, there is almost no change in OSL signals. Thus, it can be concluded that the OSL signals of natural fluorite samples are reproducible within around ± 5 per cent (1 σ standard deviation) for 100 mGy irradiation.

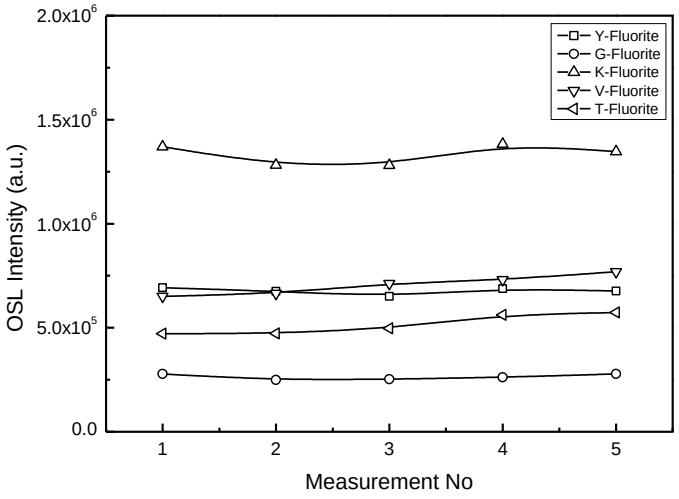

Figure 6.7 Reproducibility of the OSL signals of natural fluorites for 100 mGy β doses.

6.8 Fading Properties of the OSL Signals

High thermal stability of the OSL signal is a desired feature in radiation dosimetry applications. Therefore, there should be no fading process. To observe the fading

properties of OSL signals, the samples were kept in dark and at room temperature after irradiation with 100 mGy and the preheating. At the end of each storage period (up to 16 weeks) OSL signals were monitored. It should be noted that fading tests were performed for 5 different storage times, for each period, two aliquots were used. Thus, the normalization constant between the aliquots were taken into consideration while the variation was plotted. The variations of the OSL signals as functions of storage time are given in Fig. 6.8. According to the plots, fast decrease in a week and then slow decrease relative to the former is observed between the first and sixteenth week for each fluorite sample excluding the V-fluorite. Approximately 18% of the signal intensity of V-fluorite is faded in 16 weeks. However, for remaining samples, ~ 10% of the signals are faded in a week and then ~ 20% of the rest signals are faded between the first and the sixteenth week except that for G-fluorite. Its rest signal is decreased in an amount equal to ~ 40%. This much fading at the OSL signal is not a wanted feature in dosimetric applications. In a real life dosimetry study correction should be made.

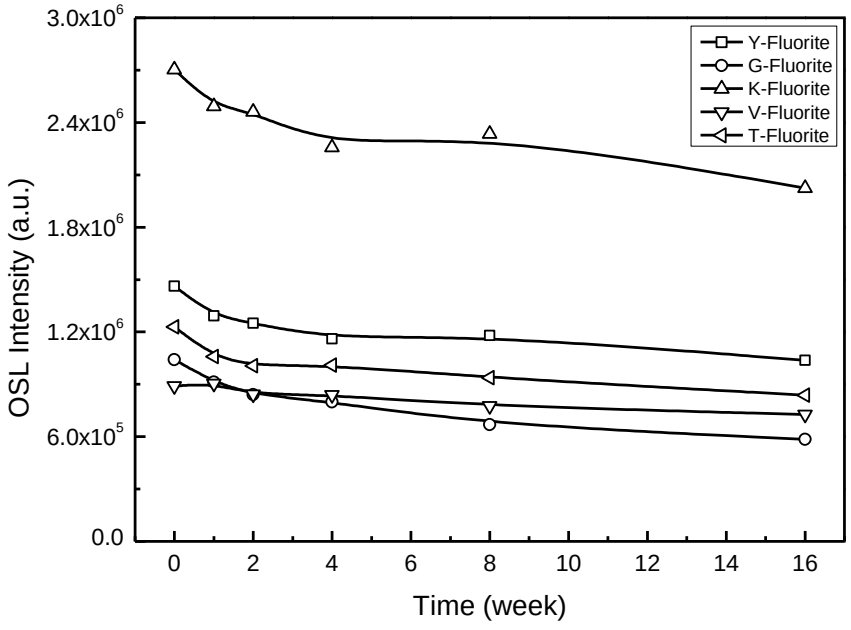

Figure 6.8 Fading of the OSL signals of natural fluorite samples.

Dosimetric properties of the OSL signals of natural fluorite samples were discussed up to now. As from here, to understand the luminescence mechanism better, the parameters of electron and hole traps which play a role in OSL signals will be discussed.

6.9 Determination of Thermal Activation Energies of Optically Active Traps

Optically active parts of the TL signals of natural fluorite samples were discussed in section 6.5. Using these results, the thermal activation energies, the thermal energy required to stimulate the trapped electrons, for the bleached peaks appearing around 190 °C in Fig. 6.5 was calculated by using the well-known initial rise method, devised by Garlick and Gibson (1948). That is to say, the initial region of bleached TL peaks up to ~ 10 % of their peak maximum were fitted to TL equation which is $I\ T \propto A\exp\ -E/kT$. This method assumes that the concentration of trapped electrons changes by only a small amount with temperature at the beginning of the TL glow peak and thus it can be regarded as constant, so that the first and the general-order TL equations are given as $I\ T \propto A\exp\ -E/kT$, where $A=ns$. Here, n is the concentration of trapped electrons and s is the frequency factor. For further detail about this method, the book by McKeever (1985) can be referred.

Thermal activation energies using this method are given in Table 6.2. For all fluorite samples, excluding K-fluorite, energies of the bleached TL peaks were found to be around 1 eV (see Table 6.2). By comparing these energies, it is probable that the optically active parts of the TL signals may be caused by electron traps having comparable activation energies for each fluorite samples excluding the K-fluorite. Activation energy of the K-fluorite was found as 1.6 eV. This value seems to be high a bit for the activation energy of a trap whose light sensitive TL peak appearing

around 190 ˚C. However, if the frequency factor has low value enough to balance this energy value, it is possible to be the energy of such trap.

Chougaonkar and Bhatt (2004) reported that TL peaks could be correlated with OSL signal components. A possible correlation for the fluorites at this study could be searched for by comparing the thermal activation energies of light sensitive TL traps and OSL traps which will be discussed later.

Table 6.2 Activation energies of first bleached peaks of the natural fluorite samples shown in Fig. 6.5.

Natural Fluorite Samples	E (eV)
Y-Fluorite	1.2
G-Fluorite	1.4
K-Fluorite	1.6
V-Fluorite	1.2
T-Fluorite	1

6.10 Various Linear Heating Rates Experiment

Various linear heating rates method was introduced by Hoogenstraten (1958) to determine the activation energies of TL traps related to TL glow peaks. Later, this method was adapted for OSL to determine the thermal activation energies of OSL traps by Li et al. (1997). The original technique relies on the shift of the peak maximum, T_m, of a TL peak by a change in heating rate. Thermal activation energy, *E*, of a TL peak is determined by plotting $\ln T_m^2/\beta$ versus $1/T_m$. The slope of such

a plot gives E/k with an intercept of $\ln E/sk$, where k is the Boltzmann constant, β is the heating rate (K/s) and s is the frequency factor (s^{-1}). The adapted technique is based on the determination of reduction rate of an OSL signal with successively increasing preheat temperatures (performed at a constant heating rate). The plot of reduction rate as a function of temperature gives the temperature dependence of the OSL signal and has a peak form (similar to a TL peak). Calculation of activation energy requires determination of such peaks obtained with preheating at various rates. The analysis of the data has the same procedures as the original technique. For more details about this method, the reported study of Li et al. (1997) may be referred.

In applying the various heating rates method, the first step was the measurement of remaining OSL signals after preheating the samples to temperatures ranging from 50 °C to 350 °C (with 10 °C steps) at various heating rates, namely 0.5, 1, 2, 3 and 4 °C/s (see Fig. 6.9). Then reduction rates of OSL signals were determined by numerical differentiation of remaining OSL versus preheat temperature curves for each heating rate. In Fig. 6.10 (a), examples of OSL reduction rate curves of V-fluorite are shown. For all samples, excluding K-fluorite, OSL reduction rate curves exhibited a single peak with maximum temperature values (for 1 °C/s) ranging between ~ 180 °C and 210 °C (see Table 6.3). For the K-fluorite OSL reduction rate curve has shown a double peak structure with maxima occurring around 210 °C and 270 °C (see Fig. 6.10 (b)).

Using the maximum temperature values, T_m, thermal activation energies and frequency factors were calculated from the slopes and intercepts of $\ln T_m^2/\beta$ versus $1/T_m$ plots as shown in Fig. 6.11. Activation energies of the four fluorite samples (excluding the K-fluorite) were found to be around 1 eV. For the K-fluorite, activation energies of the first and second peaks were determined as 0.6 and 1.1 eV, respectively (see Table 6.4).

By comparing the activation energies of the OSL traps with those of the optically active TL traps which was discussed in Section 6.9 (see Table 6.4), it was observed that these values are similar (~ 1 eV). Finally, the OSL peak temperatures were correlated with the bleached TL peak temperatures appearing around 190 °C shown in Fig. 6.5 (the second bleached peak was also considered for K-fluorite) (see Table 6.3).

In a study reported by Chougaonkar and Bhatt (2004), it has been found that traps responsible for three TL peaks appearing at 126, 196 and 264 °C with a heating rate of 5 °C/s contribute to the OSL signal of natural fluorite. Therefore, as a result, by considering the results obtained from this experiment, it can be said that TL peaks may be correlated by the OSL traps for the samples investigated in this study.

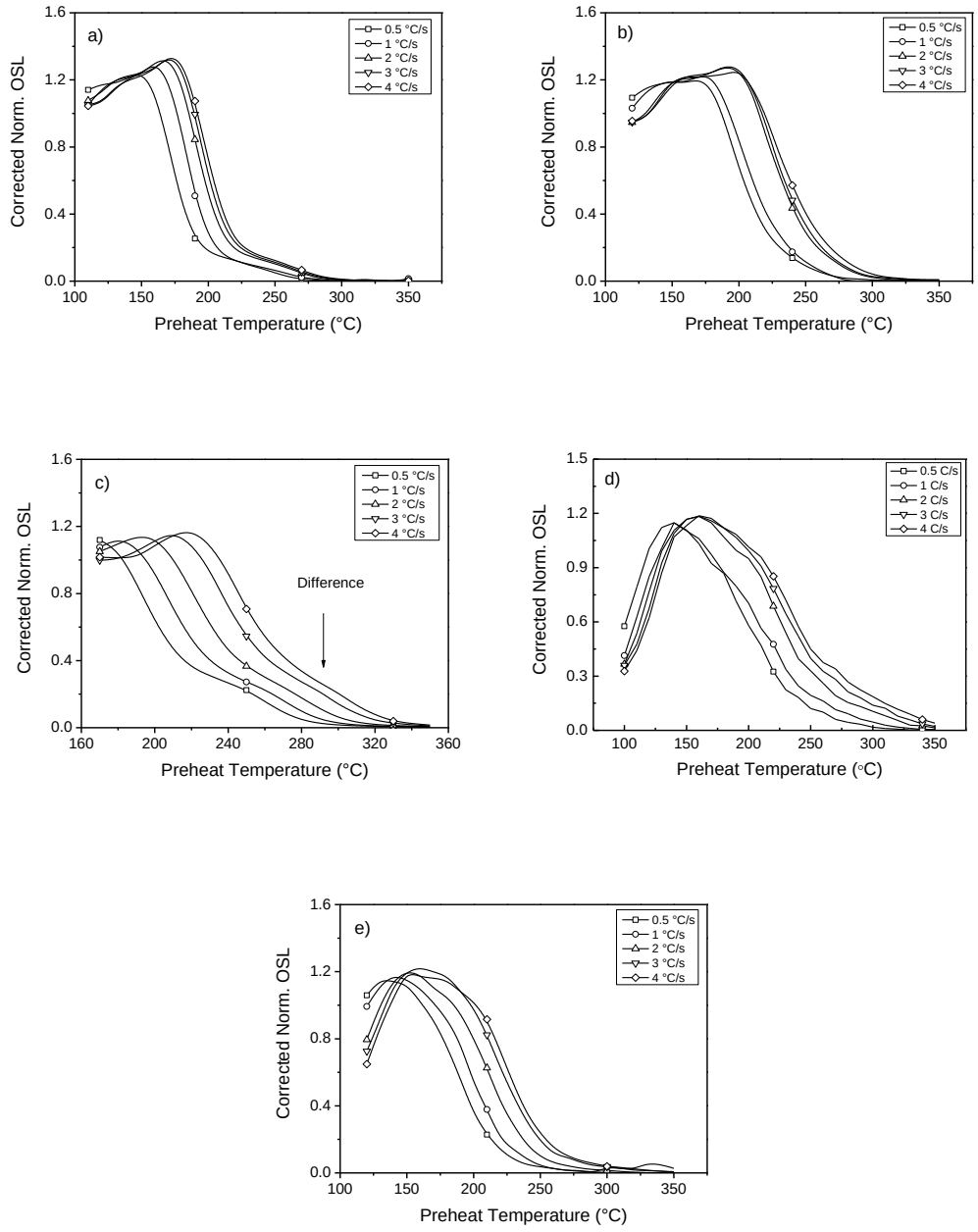

Figure 6.9 The OSL responses of the natural fluorite samples as a function of preheating temperature obtained for a different heating rates: a) Y-Fluorite; b) G-Fluorite; c) K-Fluorite; d) V-Fluorite; e) T-Fluorite.

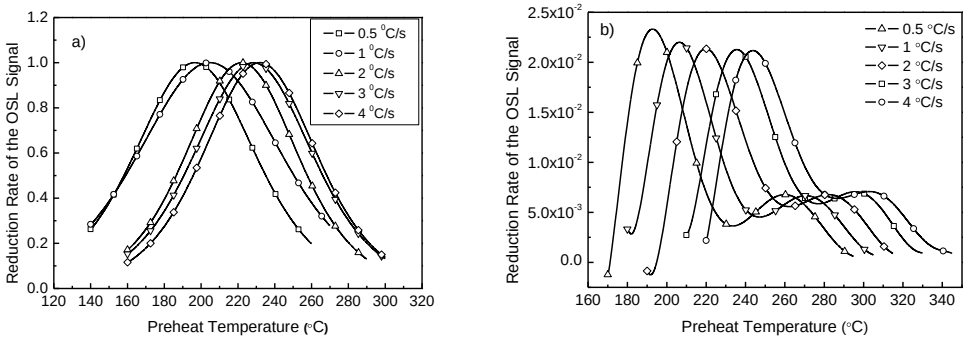

Figure 6.10 The reduction rates of the OSL signal as a function of preheat temperature for different heating rates: a) V-Fluorite, b) K-Fluorite

Table 6.3 Comparison of the OSL peak temperatures and the bleached TL peak temperatures of natural fluorite samples (for 1 °C/s heating rate).

Natural Fluorite Samples	**OSL Peak Temperatures**		**Bleached TL Peak Temperatures**	
Y-Fluorite	184 °C		187 °C	
G-Fluorite	203 °C		194 °C	
K-Fluorite	210 °C	271 °C	198 °C	295 °C
V-Fluorite	205 °C		195 °C	
T-Fluorite	197 °C		197 °C	

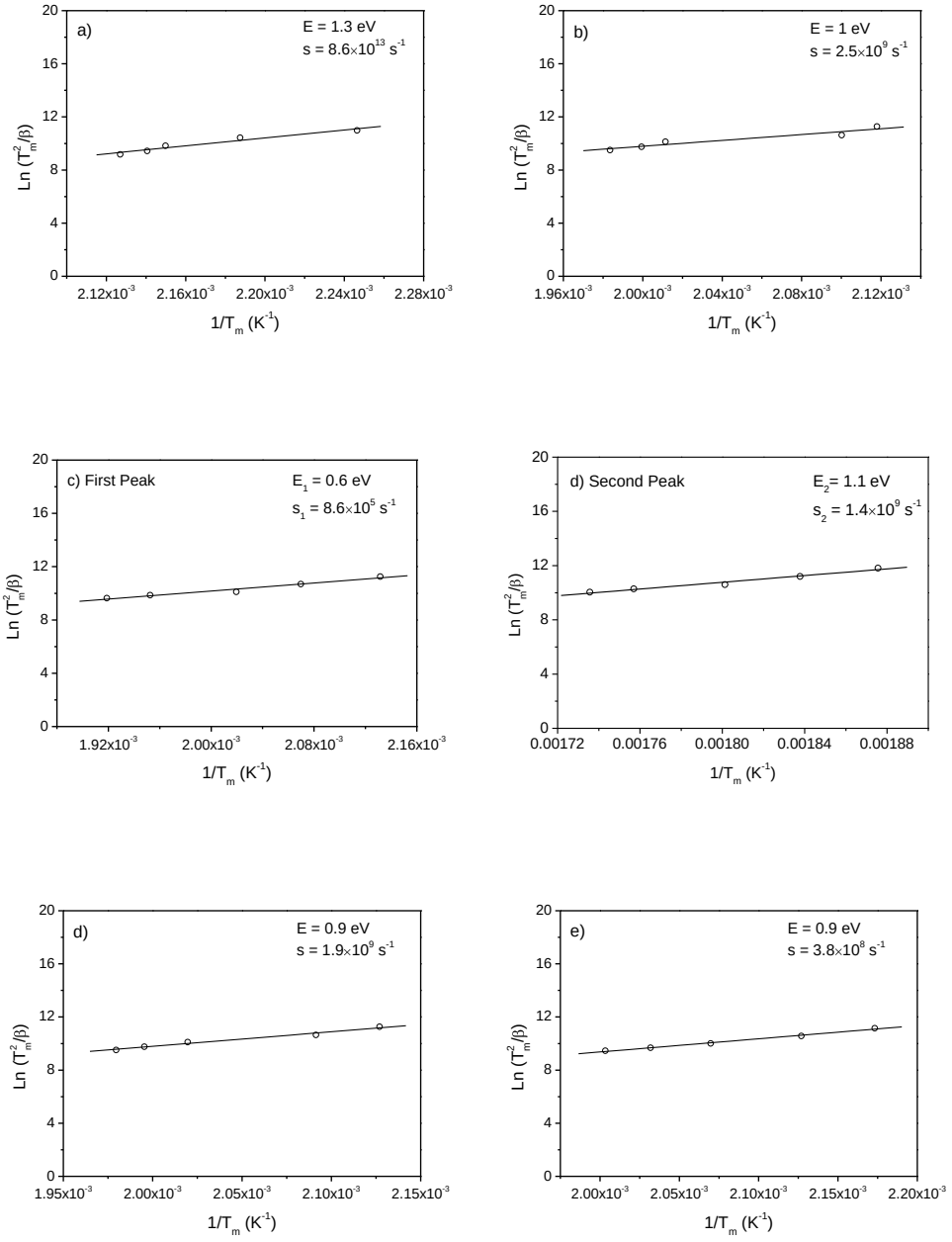

Figure 6.11 ln T_m^2/β versus $1/T_m$ plots of natural fluorite samples: a) Y-Fluorite, b) G-Fluorite, c) K-Fluorite; First peak, d) K-Fluorite; Second peak, e) V-Fluorite, f) T-Fluorite. Labels are the OSL trap parameters.

Table 6.4 Comparison of thermal activation energies of the OSL and the optically active TL traps of natural fluorite samples.

Natural Fluorite Samples	**E (eV) OSL Trap**		**E (eV) Optically Active TL Trap**
Y-Fluorite	1.3		1.2
G-Fluorite	1		1.4
K-Fluorite	0.6	1.1	1.6
V-Fluorite	0.9		1.2
T-Fluorite	0.9		1

6.11 Isothermal Decay of OSL Signals

Isothermal annealing is a well-known technique for determining the thermal activation energies of trapped charges. It relies on the determination of thermal lifetimes at various temperatures. At a fixed temperature, thermal lifetime is constant and the decay of a luminescence signal can be written as $I = I_0 \exp\ -t/\tau_T$, where I_0 is the luminescence intensity when *t=0* and τ_T is the thermal lifetime. Thermal lifetime (defined as the reciprocal of the escape probability *p*) has a temperature dependence of the form $\tau_T = \tau_0 \exp\ E/kT$. Here τ_0 is the lifetime at absolute temperature, k is the Boltzmann constant and E is the activation energy. Thus determination of τ_T at various temperatures allow one to determine the thermal activation energy using an Arrhenius plot.

Here, to have more information about the thermal activation energies of the OSL traps, isothermal decay technique is also used. To obtain isothermal decays, preheat temperatures, 150, 160, 170 and 180 ˚C, were used for different time intervals and then OSL signals were measured for 750 seconds for each time. Isothermal decay curves determined as a result of these experiments are shown in Fig. 6.12. As shown in figure, the decays are composed of two parts (Fig. 6.12) which may correspond to two different processes. The first part is between 10th and 25th minutes and the second one is between 50th and 100th minutes (see solid lines in Fig. 6.12(e)). Hence, the thermal decay constants were obtained by fitting of these two parts. Then, these decay constants were plotted as a function of preheat temperature to obtain the activation energies for two parts individually by fitting the curve to Arrhenius equation.

As a result, the thermal activation energies were found varying between 0.05 and 1 eV. These values are unexpectedly low. This may be because of retrapping effect. In the region of short time intervals (10-25 min), the retrapping probability is low during heating. Therefore, fast decay may be observed. However, in the region of long time intervals (50-100 min), the probability is increased. Hence, this may be results in slow decay. Because of these unexpected results, this experiment will be repeated in detail to obtain more reliable energy values.

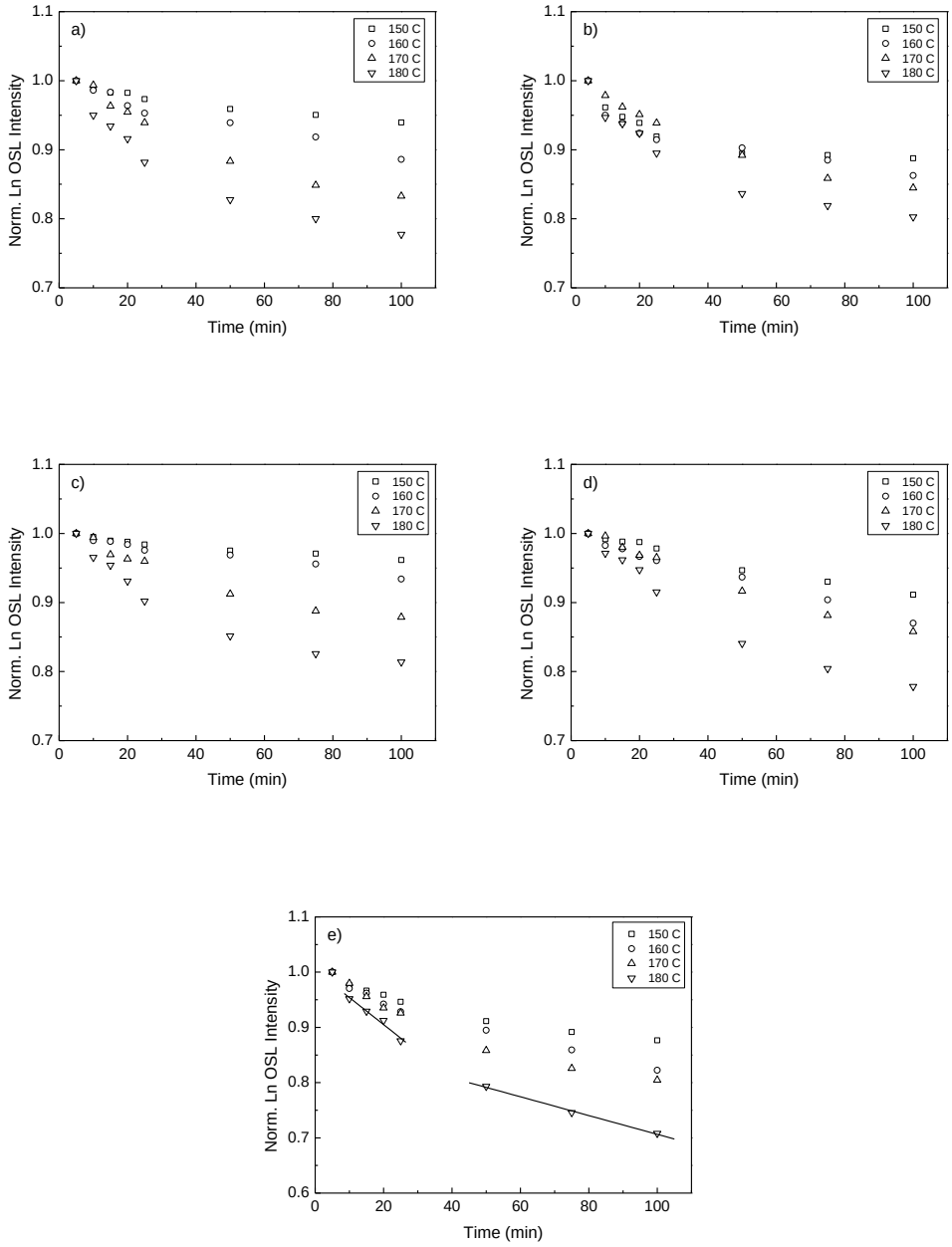

Figure 6.12 Isothermal decays of OSL signals of the natural fluorite samples for 100 mGy β doses: a) Y-Fluorite; b) G-Fluorite; c) K-Fluorite; d) V-Fluorite; e) T-Fluorite.

6.12 Thermo-Optically Stimulated Luminescence (TOL) Experiment

Thermo-Optically Stimulated Luminescence (TOL) technique, based on the measurement of OSL using brief pulses while warming up the sample, enables one to investigate the temperature dependence of the OSL production mechanisms (Duller et al., 1995). The technique can help in investigating both thermally assisted process (where an enhancement of the OSL signal is observed with increasing temperature) and thermal quenching (decrease of the luminescence efficiency with increasing temperature) of the OSL signal from the sample. Since the OSL is probed with brief pulses, measurements made using TOL is fast as it requires only one time irradiation.

TOL from fluorites were measured by heating 150 mGy irradiated and preheated aliquots to 140 ˚C at a rate of 1 ˚C/s. OSL was monitored using 0.1 second pulses at every 10 ˚C starting from 50 ˚C. A typical TOL curve is shown in Fig. 6.13. TOL curve in raw form contains both OSL and TL data, therefore to obtain the temperature dependence of OSL curves the background data (the data interval just before the OSL pulse) were subtracted from the TOL data. For five fluorite samples, measurement temperature dependence of the OSL signals are given in Fig. 6.14. As seen from the figure, OSL signal intensities were not changed significantly with temperature. These imply that neither thermal quenching nor thermal assistance is a dominant process in the OSL production mechanism.

In literature, there is no study investigating these processes for the OSL signal of natural fluorite. However, as mentioned before, Polymeris et al. (2006) have revealed the absence of thermal quenching in this mineral by observing the stability of integrals of all TL glow peaks as a function of the heating rates.

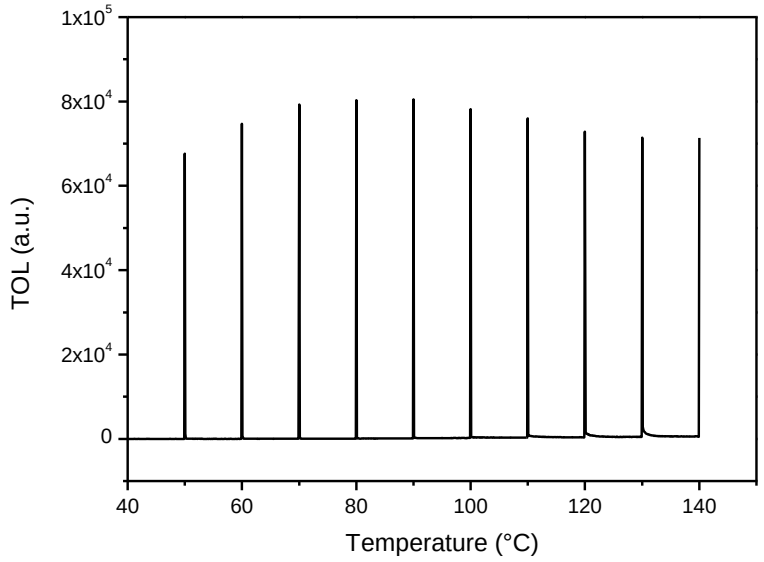

Figure 6.13 TOL signal of K-Fluorite for 150 mGy beta doses.

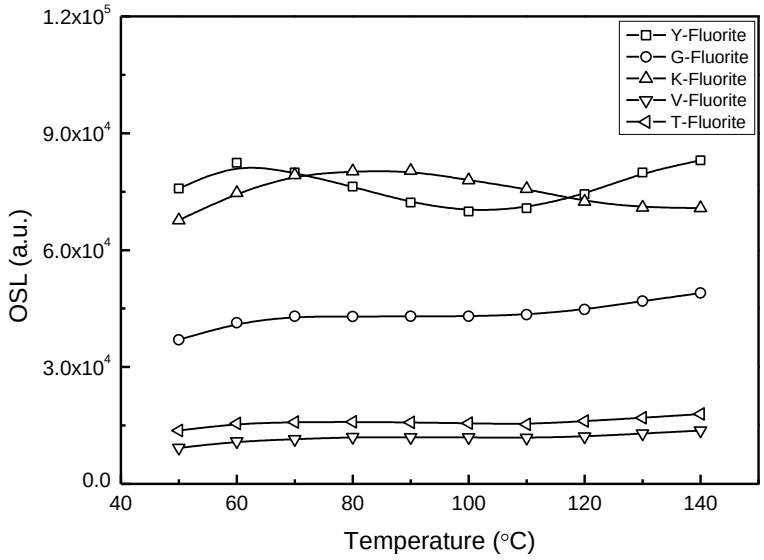

Figure 6.14 OSL versus temperature graphs of natural fluorites for 150 mGy β doses.

6.13 TR-OSL Signals

In order to gather some information about the recombination processes, TR-OSL signals of fluorites were investigated. TR-OSL from 1 Gy irradiated fluorite samples measured (at room temperature) using 100 milliseconds stimulations with 1.3107 ms intervals are given in Fig. 6.15. These signals shown in this figure show decays with lifetimes varying between 58 and 250 milliseconds. Such long recombination lifetimes imply quantum mechanically forbidden transitions. In addition to these slowly decaying signals, sudden drops in the luminescence intensities -after the cease of the stimulation light- were also observed (as demonstrated with arrow in Fig. 6.15 (a)). To explore the nature of these fast decreases in the signals, TR-OSL from the same samples were measured again using 100 nanoseconds stimulation and 5 nanoseconds data collection intervals. TR-OSL curves obtained in this manner are given as insets to plots in Fig. 6.15. Analysis of the decay curves have shown that luminescence decays could be successfully approximated with an exponential decay function of the form $I = I_0 + I_{01} \exp\ -t/\tau_r$, where τ_r is the recombination lifetime, I_0 is the background signal and I_{01} is the initial intensity. Recombination lifetimes obtained by curve fitting were found to as around 50 nanoseconds with small variations. Such fast recombination lifetime values do imply quantum mechanically allowed transitions. Thus, one may say that the luminescence signal measured in the region 300-400 nm (pass band of filter in front of the PMT) is a composite exhibiting both allowed and forbidden transitions.

More information about the luminescence production mechanism require a detailed study on spectral and time resolved measurements.

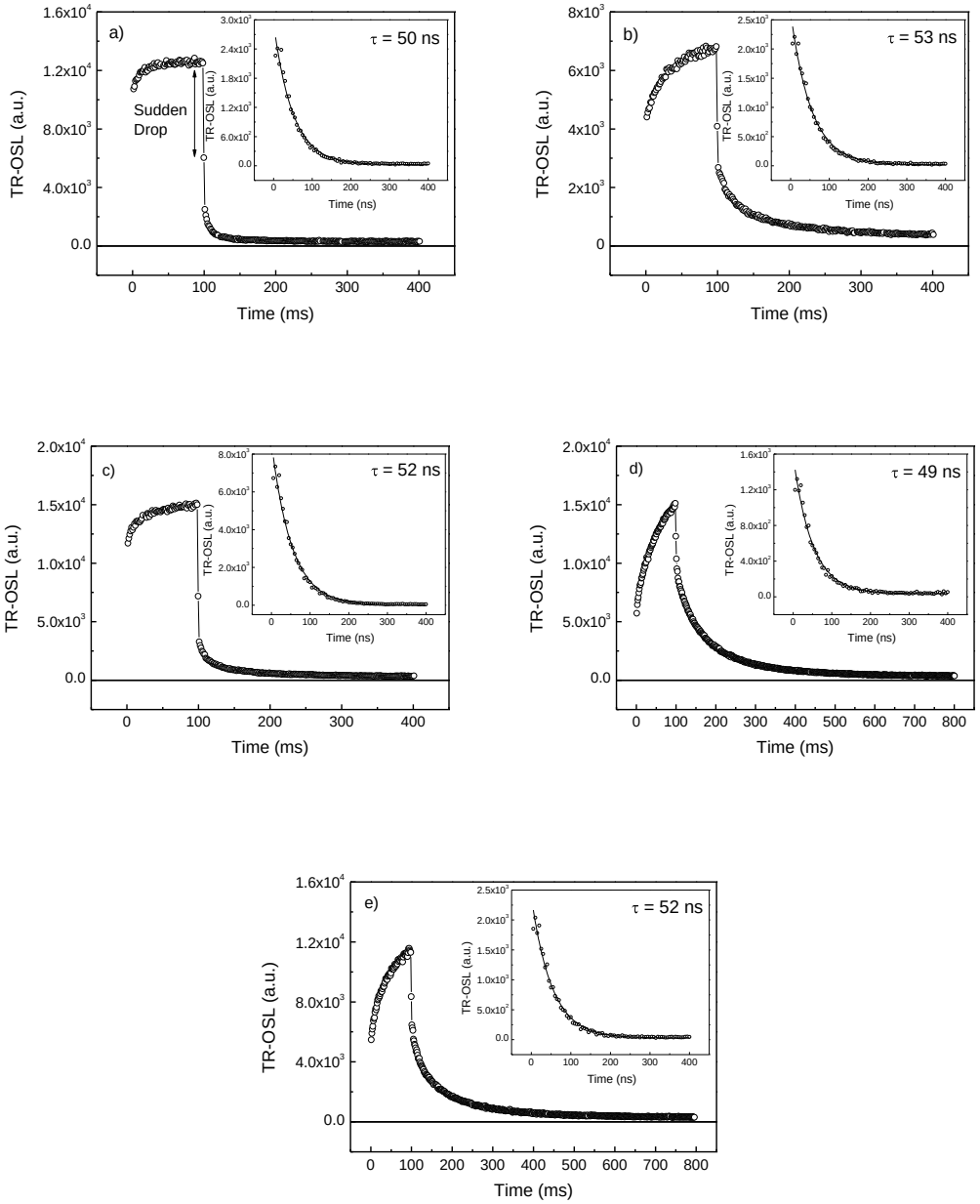

Figure 6.15 TR-OSL signals of natural fuorite samples for 1 Gy irradiation with beta doses: a) Y-Fluorite; b) G-Fluorite; c) K-Fluorite; d) V-Fluorite; e) T-Fluorite. The signals in the order of ns are shown as insets and the lifetimes obtained from them are shown as labels.

CHAPTER 7

SUMMARY AND CONCLUSIONS

Fluorites -both natural and synthetic forms- have been considered as good dosemeter materials since they have bright TL signal and high effective atomic number close to that of quartz, which make them suitable for environmental dosimetry studies. They are easily available in many places in Turkey. In addition, although thermoluminescence studies on natural fluorites are voluminous, the number of studies carried out using OSL is rather restricted (Chougaonkar and Bhatt, 2004; Polymeris et al., 2006; Yoshimura and Yukihara, 2006). All these promote an OSL study on natural fluorites devoted to develop an understanding about the luminescence signal and its behavior under various experimental conditions and also to investigate the possibility of using the material for radiation dosimetry.

OSL signals of five natural fluorite samples and their characteristics are investigated in this study. For this purpose, initially, the annealing temperature was taken as 500 ºC by considering the reported studies (Sohrabi et al., 1999; Topaksu and Yazıcı, 2007). Then, an appropriate annealing time to erase the high geological signals of the samples was found as ~ 120 hour for G-and Y-fluorite and ~ 45 hour for the rest samples. From the TL signals, post-annealing which is required for erasing the OSL signal and preparing the material for a new measurement was decided to be performed at 400 ºC for 30 minutes because it was observed that the traps related to three main TL peaks located around 100, 190 and 300 ºC were depleted at this temperature. To remove the contribution of the shallow traps from the OSL signals

preheat was performed at 150 °C for 15 minutes. These preheating parameters were determined by taking into consideration the OSL response to varying preheat temperatures and the low temperature TL peaks which are related to shallow traps.

From TL and the OSL signals obtained with experimental parameters mentioned above, it was observed that these signals have similar structure for each sample and that they are very intense which is very important feature in environmental dosimetry applications. By comparing the OSL decay constants and TL peak temperatures of five different fluorite samples, these signals are thought as caused by similar electon traps. It was also observed that TL signals are affected by OSL measurements. All TL peaks are bleached excluding the high temperature peaks of the V-fluorite and the T-fluorite. These peaks are increased after the OSL readout. This was supposed to be because of re-trapping of the charges at deeper traps during the optical stimulation which is known as phototransfer effect.

After obtaining the OSL signals, their dosimetric properties were investigated. Dose-responses of OSL signals were determined in the range 100 mGy to 100 Gy. It was observed that the samples do not have the same response. The signals of K- and Y-fluorites show linear response in the range of study. However, the signals of V- and T-fluorites have saturation doses of ~ 24 and ~ 43 Gy, respectively,. Furthermore, the G-fluorite was found to be slightly non-linear with a power factor of 1.1 instead of 1.0. According to study reported by Polymeris et al. (2006), dose response curves of natural fluorites of different origin becomes linear for doses larger than 10^{-5} Gy. If it is assumed that the samples investigated in this study have the same response, it can be concluded that natural fluorite samples have a linear response in a wide range. Also, the lowest detectable dose limit (LDDL) was also found in the order of 10^{-2} Gy for each sample assuming that the intensity corresponding to this dose is two times of the zero dose OSL reading. However, Polymeris et al. (2006) have found it as 10^{-6} Gy by defining the LDDL as the OSL signal which is higher than three standard deviations of the zero dose OSL reading. The reproducibility of the OSL signal was

tested for each fluorite sample and as a result, signals were found to be reproducible. However, fading was observed for 100 mGy irradiated samples stored in dark. Approximately 18% of the signal intensity of V-fluorite has faded in 16 weeks. For remaining samples, ~ 10% of the signals were faded in a week and then ~ 20% of the rest signals have faded between the first and the sixteenth week except that for G-fluorite. Its remaining signal was decreased by an amount equal to ~ 40%. This much fading is not a wanted feature in dosimetric applications. Nevertheless, it is possible to make corrections after investigating the fading properties of the OSL signals for different doses.

In a recent study, Chougaonkar and Bhatt (2004) have reported that TL peaks observed at 126, 196 and 264 °C correlate with components of the OSL signal. Establishing correlations between TL and OSL signal components can be helpful in developing a better understanding of the luminescence production mechanisms in the material. Thus, after studying the general properties of the OSL signals, correlation(s) between the TL and OSL signals was searched for. For this purpose, thermal activation energies of the light sensitive part of the TL signals and the OSL signals were determined using various experimental techniques. Using the initial rise method, thermal activation energies of the light sensitive TL peaks located around 190 °C were determined as ~ 1 eV for all samples excluding the K-fluorite (1.6 eV). Thermal activation energies of the OSL signals were determined using the various linear heating rates and isothermal annealing methods. The energies were found as around 1 eV which is close to the values found for light sensitive TL peaks excluding K-fluorite. For K-fluorite, that ~ 0.6 and ~ 1 eV were found which may be the energies of two different OSL traps. Also, the OSL peak temperatures appearing around 200 ˚C (temperatures corresponding to the maximum reduction rates of the OSL signals) were compared with peak temperatures of light sensitive TL peaks appearing around 190 ˚C (a second peak was also considered for K-fluorite). As a result the values were found as comparable. These results seem to support that OSL traps may be correlated with the TL signals. Isothermal decays of the OSL signals were also investigated. However, the activation energies of the OSL signals could

not be calculated well with this method because it was thought that retrapping may prevent the observation of the decay of the OSL signal by annealing time.

Experiments summarized above enable one to obtain information about the electron traps and their properties. Besides this, to have more information about the OSL production mechanisms, recombination centers and their properties should also be studied. For this purpose, temperature dependence of the OSL signals were determined using the TOL technique in which OSL was monitored using brief pulses while heating up the sample linearly. Measurements carried out in the temperature range 50-140˚C have shown that the OSL signals were not affected. This implies that the recombination centers do not suffer from thermal quenching. Furthermore, dynamics of the recombination mechanisms were studied with the help of the TR-OSL technique. TR-OSL decay curves exhibited slow (ranging between 58 and 250 milliseconds) and fast (around 50 nanoseconds) components. Existence of such slow and fast components imply quantum mechanically forbidden and allowed transitions respectively. To develop a better understanding on the recombination processes TR-OSL studies should be extended and combined with spectral measurements.

In summary, by considering the results of this study one may say that the natural fluorite samples have promising OSL properties in general to be used in environmental dosimetry applications as an OSL dosimeter. In the coming days, in order to understand the recombination mechanism thoroughly, TR-OSL signals and then, fluorescence spectra of these samples will be studied in detail.

REFERENCES

AFOUXENIDIS, D., STEFANAKI, E. C., POLYMERIS, G. S., SAKALIS, A., TSIRLIGANIS, N. C., KITIS, G., 2007. "TL/OSL Properties of Natural Schist for Archeological Dating and Retrospective Dosimetry". *Nuclear Instruments and Methods in Physics Research Section A: Accelerators, Spectrometers, Detectors and Associated Equipment*, **580**, 705-709.

AKSELROD, M. S., McKEEVER, S. W. S., 1999. "A Radiation Dosimetry Method Using Pulsed Optically Stimulated Luminescence". *Radiat. Prot. Dosim.*, **81**, 167-176.

AGULLO-LOPEZ, F., CATLOW, C. R. A., TOWNSEND, P. D., 1988. "Point Defects in Materials". Academic Press.

ANTONOV-ROMANOVSKII, V. V.,, KEIRUM-MARCUS, I. F., POROSHINA, M. S., TRAPEZNIKOVA, Z. A., 1956. "Conference of the Academy of Sciences of the USSR on the Peaceful Uses of Atomic Energy". Moscow, 1955, *USAEC Report AEC-tr-2435* (Pt. 1), 239.

ARENDS, J., 1964. "Color Centers in Additively Colored CaF_2 and BaF_2". *Phys. Stat. Sol.*, **7**, 805.

BAILIFF, I. K., 2000. "Characteristics of Time-Resolved Luminescence in Quartz". *Radiat. Meas.*, **32**, 401-405.

BAILIFF, I. K., WINTLE, A. (Ed.), 2006. "Proceedings of the 11th International Conference on Luminescence and ESR Dating Conference (2005)". *Radiat. Meas.*, **41**, 737-1050.

BAILIFF, I. K., CHEN, R., JAIN, M., LI, S. H., WALLINGA, J. (Ed.), 2009. "Proceedings of the 12th International Conference on Luminescence and ESR Dating Conference, Rome (2008)". *Radiat. Meas.*, **44**, 415-646.

BALOGUN, F. A., OJO, J. O., OGUNDARE, F. O., FASASI, M. K., HUSSEIN, L. A., 1999. "TL Response of a Natural Fluorite". *Radiat. Meas.*, **30**, 759-763.

BEAUMONT, J. H., HAYES, W., 1969. "M Centres in Alkaline Earth Fluorides". *Proc. Roy. Soc. A.*, **309**, 41-52.

BECKER, K., 1973. "Solid State Dosimetry". CRC Press.

BENNETT, H. S., LIDIARD, A. B., 1965. "The F-Centre in Fluorite Structures". *Phys. Letters*, **18**, 253-254.

BILL, H., SIERRO, J., LACROIS, R., 1967. "Origin of Coloration of Some Fluorites". *Am. Miner.*, **52**, 1003-1008.

BILL, H., CALAS, G., 1978. "Color Centers, Associated Rare-Earth Ions and the Origin of Coloration in Natural Fluorites". *Phys. Chem. Minerals*, **3**, 117-131.

BONTINCK, H., 1958. "Colour Centers in Synthetic Fluorite Crystals". *Physica*, **24**, 639-649.

BOS, A. J. J., 2001. "High Sensitivity Thermoluminescence Dosimetry". *Nucl. Instr. and Meth. B*, **184**, 3-28.

BOS, A. J. J., 2008. "Proceedings of the 15th Solid State Dosimetry (SSD15)". *Radiat. Meas.*, **43**, 131-1176.

BØTTER-JENSEN, L., 2000. "Development of Optically Stimulated Luminescence Techniques using Natural Minerals and Ceramics, and their Application to Retrospective Dosimetry". Risø National Laboratory, Roskilde

BØTTER-JENSEN, L., McKEEVER, S.W.S., WINTLE, A.G., 2003. "Optically Stimulated Luminescence Dosimetry". Elsevier, Amsterdam.

BRÄUNLICH, P., SCHAFER, D., SCHARMANN, A., 1967. “A Simple Model for Thermoluminescence and Thermally Stimulated Conductivity of Inorganic Photoconducting Phosphors and Experiments Pertaining to Infra-red Stimulated Luminescence”. *Proceedings of the First International Conference on Luminescence Dosimetry*, Stanford, June 1965, USAEC, 57-73.

BRAITHWAITE, R. S. W., FLOWERS, W. T., HAZELDINE, R. N., RUSSEL, M., 1973. “The Cause of the Colour of Blue John and other Purple Fluorites”. *Miner. Mag.*, **36**, 401-411.

BULUR, E., 1996. “An Alternative Technique for Optically Stimulated Luminescence (OSL) Experiment”. *Radiat. Meas.*, **26**, 701-709.

CALDERON, T., MILLAN, A., JAQUE, F., GARCIA SOLE, J., 1990. “Optical Properties of Sm^{2+} and Eu^{2+} in Natural Fluorite Crystals”. *Nucl. Tracks Radiat. Meas.*, **17**, 557-561.

CALDERON, T., KHANLARY, M. R., RENDELL, H. M., TOWNSEND, P. D., 1992. “Luminescence from Natural Fluorite Crystals”. *Nucl. Tracks Radiat. Meas.*, **20**, 475-485.

CHEN, R., KIRSH, Y., 1981. “Analysis of Thermally Stimulated Processes”. Pergamon Press, Oxford.

CHEN, R., McKEEVER, S. W. S., 1997. “Theory of Thermoluminescence and Related Phenomena”. World Scientific Press, Singapore.

CHOUGAONKAR, M. P., BHATT, B. C., 2004. “Blue Light Stimulated Luminescence In Calcium Fluoride, Its Characteristics and Implications in Radiation Dosimetry”. *Radiation Protection Dosimetry*, **112**, (2): 311-321.

CHITHAMBO, M. L., GALLOWAY, R. B., 2000. “A Pulsed Light-Emitting-Diode System for Stimulation of Luminescence”. *Meas. Sci. Technol.*, **11**, 418-424.

CHITHAMBO, M. L., 2003. “The Influence of Annealing and Partial Bleaching on Luminescence Lifetimes in Quartz”. *Radiat. Meas.*, **37**, 467-472.

CHITHAMBO, M. L., 2007a. “The Analysis of Time-Resolved Optically Stimulated Luminescence: I. Theoretical Considerations”. *J. Phys. D: Appl. Phys.*, **40**, 1874-1879.

CHITHAMBO, M. L., 2007b. “The Analysis of Time-Resolved Optically Stimulated Luminescence: II. Computer Simulations and Experimental Results”. *J. Phys. D: Appl. Phys.*, **40**, 1880-1889.

CLARK, R. J., BAILIFF, I. K., 1998. “Fast Time-Resolved Luminescence Emission Spectroscopy in Feldspars”. *Radiat. Meas.*, **29**, 553-560.

DANIELS, F., BOYD, C. A., SAUNDERS, D. F., 1953. “Thermoluminescence as a Research Tool”. *Science*, **117**, 343-349.

DENBY, P. M., BØTTER-JENSEN, L., MURRAY, A. S., THOMSEN, K. J., MOSKA, P., 2006. “Application of Pulsed OSL to the Separation of the Luminescence Components from a Mixed Quartz/Feldspar Sample”. *Radiat. Meas.*, **41**, 774-779.

DULLER, G. A. T., BØTTER-JENSEN, L., POOLTON, N. R. J., 1995. “Stimulation of Mineral Specific Luminescence from Multi-Mineral Samples”. *Radiat. Meas.*, **24**, 87-93.

EHRLICH, D. J., MOULTON, P. F., OSGOOD, R. M., 1979. “Ultraviolet Solid State Ce:YLF Laser at 325 nm”. *Opt. Lett.*, **4**, 184-186.

EYGİ, Z. D., EGE, O., YILMAZ, E., BULUR, E., 2007. “Development of High Power Blue and IR Stimulation Units for an OSL Measurement System”. *Balkan Physics Letters-Proceedings of TFD 24*, 224-229.

FELTHAM, P., ANDREWS, I., 1965. “Colour Centres in Alkaline Earth Fluorides”. *Phys. Stat. Sol.*, **10**, 203-211.

GAFT, M., REISFELD, R., PANCZER, G., 2005. “Luminescence Spectroscopy of Minerals and Materials”. Springer-Verlag Berlin Heidelberg.

GALLOWAY, R. B., 2002. “Luminescence Lifetimes in Quartz: Dependence on Annealing Temperature Prior to Beta Irradiation”. *Radiat. Meas.*, **35**, 67-77.

GALLOWAY, R. B., 2003. “Limestone: Some Observations on Luminescence in the Region 360 nm”. *Radiat. Meas.*, **37**, 177-185.

GARLICK, G. F. J., GIBSON, A. F., 1948. “The Electron Trap Mechanism of Luminescence in Sulphide and Silicate Phosphors”. *Proc. Phys. Soc.*, **A60**, 574.

HAYES, W. (Ed.), 1974. “Crystals with the Fluorite Structure”. Oxford University Press, Oxford.

HERCULES, D. M., 1966. “Fluorescence and Phosphorescence Analysis”. John Wiley & Sons, Inc..

HOOGENSTRATEN, W., 1958. “Electron Traps in Zinc Sulphide Phosphors”. *Philips Res. Rep.*, **13**, 515-562.

HUNTLEY, D. J., GODFREY-SMITH, D. I., THEWALT, M. L. W., 1985. “Optical Dating of Sediments”. *Nature*, **313**, 105-107.

KAISER, W., BARNET, C. G. B., WOOD, D. L., 1961. “Fluorescence and Optical Maser Effects in CaF_2:Sm”. *Phys. Rev.*, **123**, 766-776.

KAMIKAWA, T., KAZUMATA, Y., KIKUCHI, A., OZAWA, K., 1966. “The F Center in Calcium Fluoride”. *Physics Letters*, **21**, 126-128.

KAYA, Ş., 2009. “Luminescence Properties of Natural Quartz Originating from Turkey and its Usage in Retrospective Dosimetry Studies”. Master Thesis (unpublished), Ankara University, 68 pages, Ankara.

KOBAYASI, T., MROCZKOWSKI, S., OWEN, J. F., 1980. “Fluorescence Lifetime and Quantum Efficiency for 5d-4f Transitions in Eu^{2+} Doped Chloride and Fluoride Crystals”. *J. Lumin.*, **21**, 247-257.

KUBO, K., 1966. “Effects of Proton Bombardment on CaF_2 Crystals”. *J. Phys. Soc. Japan*, **21**, 1300-1303.

LEVERENZ, H. W., 1968. “An Introduction to Luminescence of Solids”. RCA Laboratories, Princeton, N.J..

LI, S., TSO, M. W., WONG, N. W. L., 1997. “Parameters of OSL Traps Determined with Various Linear Heating Rates”. *Radiat. Meas.*, **27**, 43-47.

LOH, E., 1968. “4f-5d Spectra of Rare Earth Ions in Crystals”. *Phys. Rev.*, **175**, 533-536.

LOH, E., 1969. “U.V. Absorption Spectra of Eu and Yt in Alkaline Earth Fluorides”. *Phys. Rev.*, **184**, 348-352.

MARKEY, B.G., COLYOTT, L. E., McKEEVER, S. W. S., 1995. “Time-Resolved Optically Stimulated Luminescence from α-Al_2O_3”. *Radiat. Meas.*, **24**, 457-463.

McKEEVER, S. W. S., 1985. “Thermoluminescence of Solids”. Cambridge University Press.

McKEEVER, S. W. S., MOSCOVITCH, M., TOWNSEND, P. D., 1995. “Thermoluminescence Dosimetry Materials: Properties and Uses”. Nuclear Technology Publishing.

McKEEVER, S. W. S., AKSELROD, M. S., MARKEY, B. G., 1996. “Pulsed Optically Stimulated Luminescence Dosimetry Using α-Al_2O_3:C”. *Radiat. Prot. Dosim.*, **65**, 267-272.

McKEEVER, S. W. S., CHEN, R., 1997. “Luminescence Models”. *Radiation Measurements*, **27**, 625-661.

McKEEVER, S. W. S., BØTTER-JENSEN, L., AGERSNAP LARSEN, N., DULLER, G. A. T., 1997a. “Temperature Dependence of OSL Decay Curves: Experimental and Theoretical Aspects”. *Radiat. Meas.*, **27**, 161-170.

McKEEVER, S. W. S., AGERSNAP LARSEN, N., BØTTER-JENSEN, L., MEJDAHL, V., 1997b. “OSL Sensitivity Changes During Single Aliquot Procedures: Computer Simulations”. *Radiat. Meas.*, **27**, 75-82.

McKEEVER, S. W. S. (Ed.), 2000. “Proceedings of the Ninth International Conference on Luminescence and ESR Dating Conference, Rome (1999)”. *Radiat. Meas.*, **32**, 387-880.

McKEEVER, S. W. S. (Ed.), 2003. “Proceedings of the Tenth International Conference on Luminescence and ESR Dating Conference (2002)”. *Radiat. Meas.*, **37**, 277-561.

McLAUGHLAM, S. D., EVANS, H. W., 1968. “Production of Colloidal Calcium by Electron Irradiation of CaF_2 Crystals”. *Phys. Stat. Sol.*, **27**, 695-700.

MOLLWO, E., 1934. *Nachr. Ges. Wiss. Göttingen*, **6**, 79.

MURRIETA, H., HERNANDEZ, J., RUBIO, J., 1983. “About Optical Properties of Eu Ions in Non-Metallic Crystals”. *Kinam.*, **5**, 75-121.

NAMBI, K. S. V., 1975. “Evaluation of the Absolute TL Emission Spectrum and Intrinsic Efficiency for $CaSO_4$ (Dy) and CaF_2 (Natural) Phosphors”. *Nucl. Instr. and Meth.*, **130**, 239-243.

NASCIMENTO, L. F., HORNOS, Y. M. M., 2010. “Proposal of a Brazilian Accreditation Program for Personal Dosimetry using OSL”. *Radiat. Meas.*, **45**, 51-59.

POLYMERIS, G. S., KITIS, G., TSIRLIGANIS, N. C., 2006. “Correlation Between TL And OSL Properties Of CaF_2:N”. *Nuclear Instruments And Methods In Physics Research B*, **251**, 133-142.

PRZIBRAM, K., 1956. “Irradiation Colours and Luminescence”. Pergamon Science Series, *Phys.*, **1.**

PRZIBRAM, K., 1959. “Atmosphärischer Staub und Fluoreszenz”. *Z. Phys.*, **154**, 111.

RANDALL, J. T., WILKINS, M. H. F., 1945. “Phosphorescence and Electron Traps. I. The Study of Trap Distributions”. *Proc. R. Soc.*, **A184**, 366-389.

RAO, R. P., DE MURCIA, M., GASIOT, J., 1984. “Optically Stimulated Luminescence Dosimetry”. *Radiat. Prot. Dosim.*, **6**, 64-66.

RENDELL, D., 1987. “Fluorescence and Phosphorescence Spectroscopy”. Published on behalf of ACOL, Thames Polytechnic, London by John Wiley & Sons.

ROPP, R.C., 2004. “Luminescence and the Solid State”. Elsevier, Amsterdam.

RUBLOFF, G. W., 1972. “Far-Ultraviolet Reflectance Spectra and the Electronic Structure of Ionic Crystals”. *Phys. Rev.B*, **5**, 662-684.

SANBORN, E. N., BEARD, E. L., 1967. “Sulfides of Strontium, Calcium, and Magnesium in Infra-red Stimulated Luminescence Dosimetry”. *Proceedings of the First International Conference on Luminescence Dosimetry*, Stanford, June. 1965, USAEC, 183-191.

SCOULER, W. J., SMAKULA, A., 1960. “Coloration of Pure and Doped Calcium Fluoride Crystals at 20 ˚C and -190 ˚C”. *Phys. Rev.*, **120**, 1154-1161.

Sekizinci Beş Yıllık Kalkınma Planı: Madencilik Özel İhtisas Komisyonu Raporu, “Endüstriyel Hammaddeler Alt Komisyonu Genel Endüstri Mineralleri I (Asbest – Grafit – Kalsit – Fluorit – Titanyum) Çalışma Grubu Raporu”, DPT: 2618 - ÖİK: 629, Ankara 2001, http://ekutup.dpt.gov.tr/madencil/sanayiha/oik629.pdf, Accessed on 30.11.2009.

SANDERSON, D. C. W., CLARK, R. J., 1994. “Pulsed Photostimulated Luminescence of Alkali Feldspars”. *Radiat. Meas.*, **23**, 633-639.

SHI, H., EGLITIS, R. I., and BORSTEL, G., 2005. “Ab Initio Calculations of the CaF_2 Electronic Structure and F Centers”. *Physical Review B*, **72**, 045109.

SKOOG, D. A., HOLLER, F. J., NIEMAN, T. A., 1998. “Principles of Instrumental Analysis”. Thomson Learning, Inc..

SMAKULA, A., 1954. *Z. Phys.*, **138**, 276.

SOHRABI, M., ABBASISIAR, F. and JAFARIZADEH, M., 1999. “Dosimetric Characteristics of Natural Calcium Fluoride of Iran”. *Radiat. Prot. Dosim.*, **84**, 277-280.

SUNTA, C. M., 1984. “A Review of Thermoluminescence of Calcium Fluoride, Calcium Sulphate and Calcium Carbonate”. *Radiat. Prot. Dosim.*, **8**, 25-44.

TOPAKSU, M., YAZICI, A.N., 2007. “The Thermoluminescence Properties of Natural CaF2 After Beta-Irradiation”. *Nuclear Instruments And Methods In Physics Research Section B-Beam Interactions with Materials and Atoms*, **264**, 293-301.

TSUKAMOTO, S., DENBY, P. M., MURRAY, A. S., BØTTER-JENSEN, L., 2006. “Time-Resolved Luminescence from Feldspars: New Insight into Fading”. *Radiat. Meas.*, **41**, 790-795.

URBINA, M., MILLAN, A., BENEITEZ, P., CALDERON, T., 1998. “Dose Rate Effect in Calcite”. *J. Lumin.*, **79**, 21-28.

VAGIN YU, S., MARCHENKO, V. M., PROKHOROV, A. M., 1969. “Spetrum Laser Based on Electron-Vibrational Transitions in a CaF_2:Sm Crystal”. *Sov. Phys . JETP*, **28**, 904-909.

WINTLE, A. G., 1973. “Anomalous Fading of Thermoluminescence in Mineral Samples”. *Nature*, **245**, 143-144.

WINTLE, A. G., 1975. “Thermal Quenching of Thermoluminescence in Quartz”. *Geophys. J. R. Astr. Soc.*, **41**, 107-113.

WYCKOFF, R. W. G., 1963. “Crystal Structures”. Interscience/John Wiley, New York, 9th Ed., **1**.

YELTİK, A., 2009. “Time-Resolved Optically Stimulated Luminescence (OSL) Studies on Samples Containing Quartz and Feldspar”. Master Thesis (unpublished), Middle East Technical University, 110 pages, Ankara.

YOSHIMURA, E.M., YUKIHARA, E.G., 2006. “Optically Stimulated Luminescence: Searching for New Dosimetric Materials”. *Nuclear Instruments And Methods In Physics Research Section B-Beam Interactions with Materials and Atoms*, **250**, 337-341.

YUKIHARA, E. G., GASPARIAN, P. B. R., SAWAKUCHI, G. O., RUAN, C., AHMAD, S., KALAVAGUNTA, C., CLOUSE, W. J., SAHOO, N., TITT, U., 2010. “Medical Applications of Optically Stimulated Luminescence Dosemeters (OSLDs)”. *Radiat. Meas.*, **45**, 658-662.

ZACHARIAS, N., STUHEC, M., KNEZEVIC, Z., FOUNTOUKIDIS, E., MICHAEL, C. T., BASSIAKOS, Y., 2007. “Low-Dose Environmental Dosimetry using Thermo- and Optically Stimulated Luminescence”. *Nuclear Instruments and Methods in Physics Research Section A: Accelerators, Spectrometers, Detectors and Associated Equipment*, **580**, 698-701.